Animal 20 (2026) 101823

Contents lists available at ScienceDirect

Animal
The international journal of animal biosciences

Integrative metagenomic and metabolomic profiling identifies faecal biomarkers of prolonged social stress in pigs

R. Río-López [a,1], I.-T. Vourlaki [b,1], A. Clavell-Sansalvador [b], A. Valdés [c], L. Padilla [a], L.J. García-Gil [d], X. Xifró [e], M. Ballester [b], R. Quintanilla [b], J. Ochoteco-Asensio [b], F.X. Prenafeta-Boldú [f], A. Dalmau [a], Y. Ramayo-Caldas [b,*]

[a] Animal Welfare Subprogram, Institute of Agrifood Research and Technology (IRTA), Finca Camps i Armet, Building C, 17121, Monells, Girona, Spain
[b] Animal Breeding and Genetics Program, Institute of Agrifood Research and Technology (IRTA), Road C-59, Km 12,1, Torre Marimon, 08140, Caldes de Montbui, Barcelona, Spain
[c] Department of Bioactivity and Food Analysis, Food Science Research Institute (CIAL), Spanish National Research Council (CSIC), Nicolás Cabrera 9, 28049, Madrid, Madrid, Spain
[d] Digestive Diseases and Microbiota Group, Biomedical Research Institute of Girona (IDIBGI), Parc Hospitalari Martí i Julià, Building M2, 17190, Salt, Girona, Spain
[e] New Therapeutic Targets Lab Research Group, Medical Sciences Department, Faculty of Medicine, University of Girona, Emili Grahit 77, 17071, Girona, Girona, Spain
[f] Sustainability in Biosystems, Institute of Agrifood Research and Technology (IRTA), 08140, Caldes de Montbui, Barcelona, Spain

ARTICLE INFO

Article history:
Received 6 August 2025
Revised 31 March 2026
Accepted 2 April 2026
Available online 08 April 2026

Keywords:
Gut-brain axis
Machine learning
Metabolome
Metagenome
Multiomics

ABSTRACT

Stressors significantly impact human and animal health, increasing the risk of physical and mental disorders, in part by affecting the gut-brain axis. Although a link between stress, alterations in gut microbial composition, and the serum metabolite profile has already been established in humans, multiomics studies integrating the faecal microbiome and untargeted metabolomics remain unavailable. The objectives of the present study were twofold: first, to identify microbial and metabolic signatures associated with prolonged stress, and second, to evaluate the potential of integrative multiomics approaches to predict key metabolites and discover non-invasive faecal biomarkers of stress in pigs (n = 60). Gut microbial profiles were obtained by shotgun metagenomic sequencing, while faecal metabolites were analysed by untargeted reverse-phase liquid chromatography quadrupole time of flight mass spectrometry, followed by partial least squares discriminant analysis. Metabolite prediction from microbial features was performed using the machine learning method based on neural ordinary differential equations. Eleven discriminant metabolites were identified. In the control group, neurotransmitters such as serotonin and metabolites such as 2-acetamidophenol and sinapine (which possess anti-inflammatory and antioxidant properties) were the most prominent. Conversely, the stressed group exhibited elevated levels of xanthosine, pyrimidine bases (thymine and uracil), n-octadecylamine, and N-α-acetyl-L-lysine. N-octadecylamine (r = 0.37) showed a positive, and serotonin (r = −0.32) a negative correlation with hair cortisol. The results revealed interspecific interactions that modulated microbial and metabolic shifts between the control and stressed pig groups. Feature selection further identified 64 microbial genes that improved classification accuracy between control and stressed pigs to 91.06% and enhanced the prediction of key metabolites, including serotonin and xanthosine. Overall, this integrative multiomics framework elucidates complex microbiome-metabolite interactions and identifies non-invasive biomarkers of prolonged stress-induced metabolic dysregulation, providing valuable insights for animal welfare and translational human health research.

Implications

Prolonged stress poses a major challenge to pig production, yet its impact on the gut microbiome and its metabolic outputs remains poorly understood. This study investigated how chronic social stress alters the faecal microbiome and metabolome in pigs, integrating multiomics data to identify potential non-invasive biomarkers. We identified condition-specific metabolites, including serotonin and xanthosine, and demonstrated that metagenomic data can accurately predict relevant metabolites. These findings highlight a set of candidate faecal biomarkers that could support the monitoring of animal welfare in commercial settings, offering a practical approach for the early detection of stress-induced disturbances.

* Corresponding author.
E-mail address: yuliaxis.ramayo@irta.cat (Y. Ramayo-Caldas).
[1] Equal contributions.

https://doi.org/10.1016/j.animal.2026.101823
1751-7311/

Introduction

The intensification of modern animal production systems, driven by growing global food demand, has made stress management a critical challenge for pigs, as chronic stress significantly compromises welfare and productivity (Martínez-Miró et al., 2016). Among stressors in pig production, social stress resulting from regrouping and crowding is particularly relevant (Turner et al., 2000; Proudfoot and Habing, 2015; Fu et al., 2016). Pigs are highly social animals (Meese and Ewbank, 1973), and the destabilisation of their hierarchies induces acute stress responses (Galli et al., 2023), while prolonged spatial restriction promotes chronic stress through sustained competition for resources, especially during later growth stages (Camp Montoro et al., 2021; Nannoni et al., 2019). Stress responses influence host physiology and behaviour through the Microbiota-Gut-Brain Axis (**MGBA**), a multifaceted system that comprises the gut microbiota (Leigh et al., 2023), the immune system (Ravi et al., 2021), and the central nervous system (Principi and Esposito, 2016; Russell and Lightman, 2019). These management-related stressors, therefore, provide a suitable biological model to investigate how persistent psychosocial challenges perturb this axis.

In swine, stress has been reported to cause immune dysfunction (Gimsa et al., 2018), metabolic alterations (Sánchez et al., 2022; Tang et al., 2022), and increased disease susceptibility (Kick et al., 2011). In particular, accumulating evidence indicates that stress induces marked shifts in gut microbial structure and function (Li et al., 2018; Vourlaki et al., 2025). However, stress and the gut microbiome are engaged in a dynamic, bidirectional relationship rather than a unidirectional cause-and-effect process. Gut microbiota actively contributes to the MGBA by producing bioactive compounds (Silva et al., 2020; Vasquez et al., 2022; Zhou et al., 2023), such as short-chain fatty acids, amino acid derivatives, and neurotransmitter-like molecules, which influence the hypothalamic–pituitary–adrenal axis and host behaviour.

Despite the wide range of stress-related effects, blood cortisol is the primary and most widely used stress biomarker (Martínez-Miró et al., 2016). Even so, non-invasive samples such as saliva, faeces and hair are increasingly preferred in pig welfare studies (Escribano et al., 2015; Prims et al., 2019; Svoboda et al., 2024). Saliva and blood cortisol mainly reflect acute stress (Svoboda et al., 2024), whereas hair cortisol integrates long-term hormonal exposure and is better suited to evaluate chronic stress (Heimbürge et al., 2019). Nevertheless, assessing stress solely through unique endocrine biomarkers cannot capture the complexity of the MGBA dialogue under stress exposure. Given the diverse causes and multiple physiological systems involved in the stress response, a range of biomarkers should be considered (Papatsiros et al., 2024). Emerging evidence suggests that a multibiomarker approach that integrates host, microbial and metabolic information may better characterise stress-induced dysregulation (Menneson et al., 2019; He et al., 2021; Clavell-Sansalvador et al., 2024).

The identification of non-invasive stress biomarkers could facilitate the early detection of welfare disturbances in pigs (Zheng et al., 2024; Li et al., 2018) and might aid in developing interventions for stress-related human disorders, including major depressive disorder (Valles-Colomer et al., 2019; Liu et al., 2024). Recent advances in omics technologies, such as metagenomics and untargeted metabolomics, have provided tools for investigating stress-induced effects on the MGBA and its related pathways. Several studies have linked stress and depressive disorders to altered gut microbial composition (Nguyen et al., 2023; Zhao et al., 2024; Clavell-Sansalvador et al., 2024) and to changes in serum metabolite profiles (Amin et al., 2023). However, the faecal metabolites and the microbial taxa associated with these processes remain poorly understood. Moreover, most studies have focused on isolated gut microbiota components or metabolic pathways, with limited attempts to integrate multiomics data into intricate gut microbiome-metabolome interactions. Such integrative strategies would enable the joint interpretation of microbial composition, functional capacity, and metabolite production in the context of host physiology, offering a comprehensive framework for investigating host-microbial interactions under stress conditions.

To address these gaps, the present study examined alterations in microbial communities and faecal metabolites induced by prolonged social challenge, integrating shotgun metagenomics and faecal untargeted metabolomics in a porcine stress model. The objective was to identify the microbial and metabolic signatures associated with the social stress response and provide insight into how chronic stress influences the gut microbiome and its metabolic outputs.

Material and methods

Study design

Animal care and experimental procedures were performed following the national and institutional guidelines for Good Experimental Practices and were approved by the Institute of Agrifood Research and Technology (**IRTA**) Ethical Committee, code 10329. A total of 60 Duroc pigs (30 immunocastrated males and 30 females) of the same Duroc genetic line (*Selección Batallé*) were allocated at two months of age to the IRTA experimental farm in Monells (Girona, Spain). Upon arrival, pigs were tagged and weighed. Subsequently, the animals were grouped and distributed into eight pens, each containing eight individuals (four immunocastrated males and four females), within the same building. Animal allocation followed a blocked design based on BW and lineage to homogenise pens at the start of the experiment and avoid initial bias. The experimental treatments (control vs stress) were applied at the pen level. Therefore, the pen was treated as the experimental unit for all analyses of treatment effects. Pigs in the stress group were subjected to more stressful conditions than those in the control group. First, their space was restricted to the legal minimum of 1 m^2 per pig at the end of the growing period, thereby increasing resource competition, whereas the control group received 1.5 m^2. Furthermore, to disrupt social hierarchies and incite conflict to re-establish the dominance order, the stress group underwent two additional mixing events compared with the control group. Firstly, there was an initial mixing while allocating all the animals in their original pens, followed by a second mixing event two months later, during which all females from different stress pens were mixed, and a final mixing event three weeks later, involving the mixing of male animals. Throughout these procedures, animals were consistently housed in pens with unfamiliar individuals, and the control group remained unaltered. During the experimental period, the animals received a cereal-based diet formulated to meet the nutritional requirements for each period (Nutrient Requirements of Swine, 2012), detailed in Supplementary Table S1. Although treatments were applied at the pen level, with each pen containing only animals from a single treatment, individual measurements, including BW, feed intake, hair cortisol concentration, and faecal samples, were collected from each animal. As described by Clavell-Sansalvador et al. (2024), individual feed intake (Nedap electronic feeding stations) and BW were recorded to calculate the average daily gain, feed conversion ratio, and residual feed intake. At the end of the growing period (seven months of age), hair and faecal samples were collected in an experimental slaughterhouse for cortisol analysis,

shotgun metagenomic, and metabolomic profiling (Fig. 1). Specifically, hair was obtained from the fronto-parietal region of the pig's head using an electric clipper. It was stored in zipper bags in the absence of light at −80 °C. Faecal samples were collected directly from the rectum of each animal using sterile disposable gloves. Contact with the ground was avoided to minimise environmental contamination, and gloves were changed between animals to prevent cross-contamination. The samples were immediately stored at −80 °C in two 4 mL cryotubes per animal.

Microbial DNA extraction and shotgun metagenomics sequencing

Total DNA from 250 mg of faeces was extracted using the DNeasy PowerSoil Pro kit (QIAGEN, Tegelen, the Netherlands) following the manufacturer's instructions and quantified using the Qubit dsDNA Broad Range assay kit (Thermo Fisher Scientific). Shotgun metagenomic libraries were prepared at the Centre for Genomic Regulation (Barcelona, Spain). Library preparation was performed on a TECAN Fluent automated platform using a custom protocol based on a home-engineered Tn5 transposase (R27S, E54K, L372P). Genomic DNA was quantified using the dsDNA PicoGreen assay (Invitrogen) and normalised to 0.4 ng/μL. One nanogram of input DNA was subjected to tagmentation, simultaneously fragmenting the DNA and incorporating adapter sequences. Libraries were then amplified by limited-cycle PCR using KAPA HiFi HotStart ReadyMix (Roche; KK2601) and unique dual-index Nextera primers. PCR products were purified with in-house magnetic beads. Final libraries were evaluated for concentration and fragment size distribution using a Bioanalyzer or Fragment Analyser High Sensitivity assay (Agilent Technologies) and pooled equimolarly before sequencing. Paired-end sequencing (2 × 150 bp) was performed on a single Illumina NovaSeq 6000 platform at a sequencing depth of ~10 Gb per sample.

Computational analysis of metagenomics

Bioinformatic analysis includes taxonomic profiling, generation of Metagenome-Assembled Genomes (**MAGs**), microbial gene inference, and functional prediction. Initially, the nf-core/mag 2.5.1 pipeline (Ewels et al., 2020; Krakau et al., 2022) was employed to perform quality control and host decontamination by removing reads that mapped to the porcine *Susscrofa11.1* assembly genome. Then, the remaining reads were processed following complementary approaches: (1) taxonomic profiles were obtained by performing read-based classification on unassembled reads using sylph v0.8 (Shaw and Yu, 2023) against the GTDB-R220 database (release 09-RS220, 24 April 2024); and (2) individual sample assemblies were generated using Megahit v1.0.2 (Li et al., 2015) as implemented in the nf-core/mag pipeline. Binning was performed with nf-core/mag using MaxBin2 (Wu et al., 2016) and MetaBAT2 (Kang et al., 2019). The resulting bins were refined with the bin refinement module of metaWRAP (Uritskiy et al., 2018) and dereplicated with dRep v3.5.0 (Olm et al., 2017). The parameters for the refinement module were set at a minimum completion of 70% (*-c 70*) and a maximum contamination of 10% (*-x 10*). Completeness and contamination of each MAG were assessed using CheckM2 (Chklovski et al., 2023). Taxonomic annotation of the resulting MAGs was performed using GTDB-Tk v2.4.0 (Chaumeil et al., 2020), and their functional annotation was performed with DRAM (Shaffer et al., 2020) against the PFAM-A, KOfam, and dbCAN-V10 databases (downloaded in July 2024). The R package 'distillR' was used to transform the DRAM annotations of each MAG into multiple Genome Inferred Functional Traits (Kanehisa and Goto, 2000; Alberdi, 2022). Finally, the mapping rate of metagenomic reads, MAGs, and gene abundance was calculated using coverM (Aroney et al., 2024).

Metagenomic statistical analysis

To identify the microorganisms that better discriminate between stress and non-stress conditions, Partial Least Squares Discriminant Analysis (**PLS-DA**) was applied to Centred Log-Ratio (**CLR**)-transformed MAG abundances using the mixOmics R package v6.30.0 (Rohart et al., 2017). Because log-ratio transformations cannot be computed in the presence of zeros, all CLR-transformed tables in our analyses were first adjusted by adding a small pseudocount (0.0001) to each feature to handle zero values. Model robustness was evaluated through 10 000 iterations of cross-validation, with the dataset randomly partitioned into 70% training and 30% testing subsets per iteration. Predictions were generated using Mahalanobis distance, and the resulting confusion matrices were aggregated to compute overall accuracy, class-specific performance metrics, and error rates. The optimal number of components was chosen as the one yielding the lowest balanced error rate for Mahalanobis distance, determined via 4-fold cross-validation repeated 100 times. The discriminative MAGs were identified based on Variable Importance in Projection (**VIP**) scores using the vip() function from the R package mixOmics. Variables with VIP > 1 were considered important contributors to the discrimination between groups.

Cortisol extraction and quantification

To assess chronic stress, cortisol was extracted from hair at the end of the experiment using the method described by Davenport et al. (2006). Briefly, 250 mg of hair was weighed, placed in a polypropylene tube, and washed with five millilitres of isopropanol. After mixing at room temperature and centrifugation at 1 500 g for 1 min, isopropanol was discarded, and the washing step was repeated. The samples were left to dry completely at room temperature before being cut into small pieces (~5 mm). Subsequently, 60 mg of hair from each sample was weighed, pulverised into a fine powder using a Precellys Evolution homogeniser (Bertin Technologies, France), and incubated with one millilitre of methanol for 18 h at room temperature with continuous gentle agitation for steroid extraction. The samples were centrifuged at 2 000 g for 5 min, and 0.6 mL of the methanol extract was aliquoted into a new Eppendorf tube. The extracts were evaporated to dryness using a Speed Vac Concentrator (Concentrator 5301, Eppendorf), reconstituted with 0.1 mL of phosphate-buffered saline, and stored at −80 °C until analysis. A sensitive assay based on AlphaLISA® technology (PerkinElmer), previously validated for pig hair, was used to measure cortisol in all samples. The results were expressed as pg/mg of hair. The assay showed a coefficient of variation of < 12%, with a limit of blank at 1.42 ng/mL and a limit of quantification of 6.96 pg/mL.

Metabolomic sample preparation and analysis

The metabolomic analysis was performed at the Institute of Food Science Research (CIAL-CSIC, Madrid). Stool samples were collected simultaneously as faecal samples employed in metagenomics, immediately frozen with liquid nitrogen, and stored at −80 °C. Prior to extraction, samples were homogenised by vortexing for 1 min, and one millilitre of each suspension was transferred into Eppendorf tubes. Samples were dried in a SpeedVac concentrator without heating for 7.5 h. Subsequently, 100 mg of each dried sample was weighed and extracted with precooled 80% (v/v) methanol to a final concentration of 100 mg/mL. The Mixtures were shaken in a Thermomixer at four degrees Celsius and 2 000 rpm for 10 min, followed by 30 min of ultrasonication at

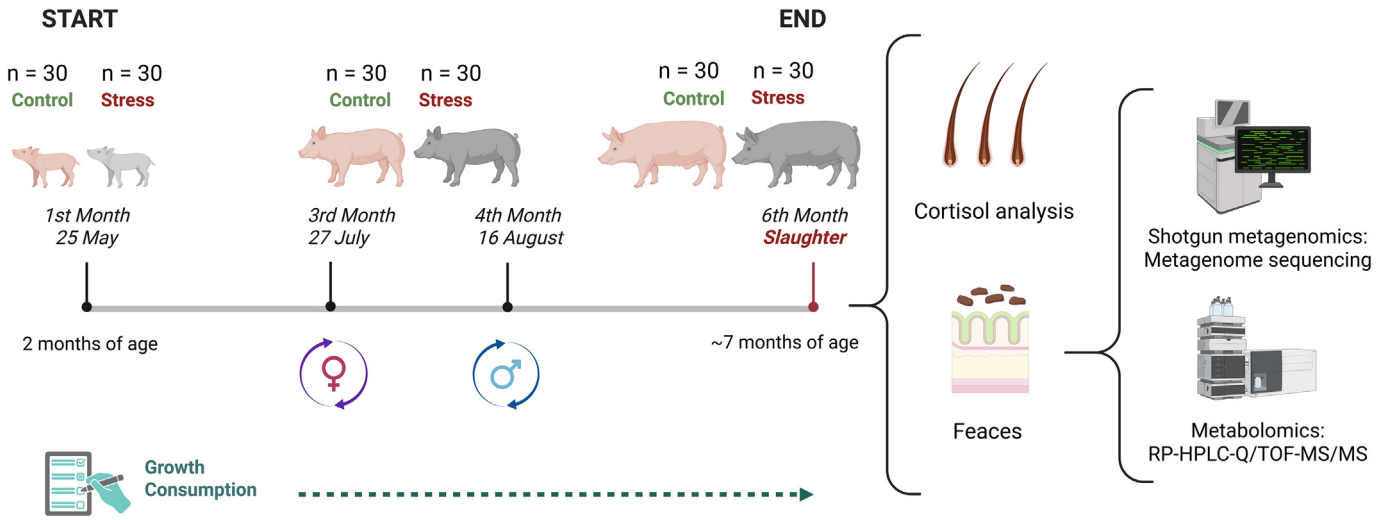

Fig. 1. Experimental timeline and study design. Schematic representation of the experimental design involving sixty two-month-old Duroc pigs (30 immunocastrated males and 30 females) assigned to control (n = 30) or stress (n = 30) treatments at the pen level (eight pigs per pen, balanced by sex). The stress treatment combined reduced space allowance (1 m^2 vs 1.5 m^2) and repeated social mixing to induce chronic stress and increase social instability, whereas control animals remained under standard housing conditions. Growth performance was monitored during the growing period. At seven months of age, hair and faecal samples were obtained for cortisol quantification, gut microbiome characterisation (shotgun metagenomics), and untargeted faecal metabolomic analysis. Created in BioRender (https://BioRender.com/s92t971). Abbreviations: RP-HPLC-Q/TOF-MS/MS = untargeted reverse-phase liquid chromatography quadrupole time of flight mass spectrometry.

room temperature. Samples were then shaken again for 5 min under the same Thermomixer conditions and centrifuged at 14 800 rpm for 15 min at four degrees Celsius. The supernatants were collected and stored at −80 °C until Reverse-Phase Liquid Chromatography Quadrupole Time Of Flight Mass Spectrometry (**RP-HPLC-Q/TOF-MS/MS**) analysis.

A sample volume of two microlitres was injected (three technical replicates) into an HPLC model 1290 (Agilent Technologies, Germany). The chromatographic separation was performed on Agilent Zorbax Eclipse Plus C18 analytical column (100 × 2.1 mm inner diameter; 1.8 µm particle size) equipped with an Agilent Zorbax C18 precolumn (5 × 2.1 mm inner diameter, 1.8 µm particle size) with Milli-Q water (A) and acetonitrile (B) acidified by 0.1% (v/v) formic acid as the mobile phase at flow rate of 0.5 mL/min at 40 °C. The mobile phase gradient started at 0 min with 0% (B), 0–30% (B) in 7 min, 30–80% (B) in 2 min, 80–100% (B) in 2 min, 100% (B) in 2 min, 100–0% (B) in 1 min, and 0% (B) in 3 min to come back to initial conditions. Compounds were eluted into a Q/TOF series 6540 from Agilent Technologies (Germany), equipped with an Agilent Jet Stream thermal orthogonal ESI source. The mass spectrometer was operated in ESI positive mode using the following parameters: capillary voltage, 3 000 V; mass range, 25–1 100 *m*/*z*; nebulise pressure, 40 psig; drying gas flow rate, 8 L/min; dry gas temperature, 300 °C. The sheath gas flow was 11 L/min at 350 °C. Method blanks and a pooled mixture of all samples (20 µL of each) were included as quality control samples and were subjected to iterative MS/MS with a mass error tolerance of 20 ppm and retention time exclusion tolerance of ± 0.2 min to increase the coverage of the MS/MS spectra acquired. MS/MS spectra were acquired employing the auto MS/MS mode using five precursors per cycle, dynamic exclusion after two spectra (released after 0.5 min), and collision energies of 20 and 40 V. Mass accuracy was corrected using ions at *m*/*z* 121.0509 (C5H4N4) and 922.0098 (C18H18O6N3P3F24) simultaneously pumped into the ion source.

MicrobeMASST

To investigate the potential relationship between the faecal microbiome and discriminant metabolites, an *in silico* analysis was performed using MicrobeMASST v. 2025.03.25, a recent taxonomically informed mass spectrometry search tool for microbial metabolomics (Zuffa et al., 2024). MicrobeMASST databases provide metabolite annotations for untargeted metabolomics experiments, based on a curated database of over 60 000 microbial monocultures (Zuffa et al., 2024). Therefore, allowing users to compare experimental MS/MS spectra with reference microbial spectra to associate annotated metabolites with putative microbial producers based on similarity in MS/MS fragmentation patterns.

Untargeted metabolomics data processing and analysis

Data obtained from RP-HPLC-Q/TOF-MS/MS were converted to ABF format and processed by MS-DIAL software v. 4.9.221218 using the same parameters as those used by Valdés et al. (2022). All metabolites were annotated following the Metabolomics Standard Initiative guidelines (Sumner et al., 2007) as level 2a (metabolites with precursor *m*/*z* and MS/MS spectral library matching). The list of metabolites was filtered by removing unknown metabolites, metabolites with a maximum peak height less than three times the average height in the method blanks, and metabolites with a maximum height less than one thousand units. Missing values were imputed by half of the minimum height value, the median of the three technical replicates was calculated, and the data were processed using the bioinformatic tool MS-FLO (https://msflo.fiehnlab.ucdavis.edu/). Duplicated metabolites and isotopes were removed, the heights of the different adducts from the same compound were combined, and Systematic Error Removal using the Random Forest normalisation method (Fan et al., 2019) was applied using the pool mixtures as reference samples.

Metabolite discriminant analysis

The resulting tentative metabolite profiles were transformed using the Additive Log-Ratio (**ALR**) transformation, as follows:

$$ALR(\mathrm{j}|\mathrm{ref}) = \log\left(\frac{x_j}{x_{ref}}\right) = \log(x_j) - \log(x_{ref})$$

where the number of total ALR is *j-1*, j is the total number of tentative metabolites (n = 114), *xref* is the reference variable (C8H9NO4) with the lowest variance (0.0187) and the highest Procrustes correlation score (0.997; Greenacre et al., 2021). Supplementary Table S2 summarises these statistics for all 114 features. The ALR-transformed data were auto-scaled, and PLS-DA was employed to select metabolites that optimally discriminated between control and stressed pigs (Rohart et al., 2017). The optimal number of components was determined by selecting the lowest balance error rate for Mahalanobis distance through 4-fold cross-validation, repeated one hundred times. Afterwards, only the tentatively identified metabolites with a VIP score > 1 were retained for a subsequent PLS-DA model. Ultimately, the classification performance of the final model (based on the selected variables) was validated using a confusion matrix, employing 4-fold cross-validation repeated 10 000 times, as previously described by Casto-Rebollo et al. (2023). The metabolites retained in the final PLS-DA model were correlated with hair cortisol concentrations, the abundance of discriminant MAGs and the abundance of genes selected by the procedure described in the following sections, using Pearson's correlation coefficient ($P < 0.05$).

Metabolomic predictions and microbiome-metabolites interactions

The discriminant metabolite profiles were predicted from microbial abundance using the machine learning method based on Neural Ordinary Differential Equations (**mNODE**; Wang et al., 2023a). This method incorporates neural ordinary differential equations in a multilayer perceptron neural network as a module in the middle-hidden space, between two fully connected layers. In this way, the model uses relative microbial abundance as input to predict discriminant metabolite profiles as output.

First, the entire dataset was split into training (80% records) and test (the remaining 20% records) datasets. The CLR transformation was then applied to the microbial abundance and metabolite tables. The mNODE was applied to the training set following a 5-fold cross-validation strategy to define the optimal hyperparameters. Once optimised and retrained on the training set with the best hyperparameters, the model was used to predict the CLR-transformed metabolomic profiles of the test dataset. As proposed by Wang et al. (2023a), the Spearman correlation coefficient (ρ) between the predicted and observed CLR-transformed metabolic profile was used as the evaluation metric.

An additional concept implemented by the mNODE approach is the inference of microbe-metabolite production and consumption interactions, which was considered a measure of the susceptibility of the metabolite to the microbe abundance. This metric reflects the association between the abundance of a microbial trait (at the taxonomic or gene level) and a metabolite. The method applies small perturbations in the microbial relative abundance, inferring the response of metabolite abundance to these changes for each metabolite-microbe pair. Particularly, the influence of specific species on metabolite *a* is measured as the perturbation of the relative abundance of species *i* (x_i) by a small amount (Δx_i) applying the trained mNODE to re-predict the concentration of metabolite *a* and then calculate the deviation from the original prediction (Δy_a). The susceptibility of metabolite *a* to species *i* is defined as: $s_{ai} = (\Delta y_a)/(\Delta x_i)$, where s_{ai} indicates the effect of species *i* on metabolite *a*. If the value is negative, suggest that a higher abundance for species *i* leads to a lower predicted concentration for metabolite α and the metabolite is likely consumed by that species. Similarly, if the value is positive, it indicates the possible production of metabolite α by species *i*. For a more detailed description of the method, see Wang et al. (2023a).

Metabolite prediction from different microbial abundance profiles

The previously described process was implemented to predict the eleven discriminant metabolites using four abundance tables derived from metagenomic data: (1) genus-level profile and (2) species-level profile, both obtained via a taxonomic reference-based approach; and (3) MAGs abundance and (4) microbial gene profile (genes), obtained through a metagenome-assembly approach. For microbial gene profile, due to the large number of variables (310 192 genes), an exploratory analysis was performed beforehand to identify the most informative microbial genes based on their associations with experimental conditions (control vs stress) as follows:

Frequency-based selection: Genes were selected based on the frequency differentiation comparing the control vs the stress groups of animals. The frequency of each gene was calculated for the control and stress groups. Then, eleven genes with frequency <10% in one group and >40% in the other were selected.

Feature-based selection with LASSO: LASSO (Tibshirani, 2011) is a machine learning method that is used in regression analysis. LASSO regression overcomes issues such as multicollinearity and overfitting by applying restrictions on the absolute value of the solutions (L1 norm) and performing variable selection. LASSO aims to minimise the cost function by reducing the absolute values of the coefficients; in this way, it performs automatic feature selection by discarding redundant features. The LASSO solution was defined as the set of genes that optimise the following problem:

$\widehat{\beta}(lasso) = \sum_{i=1}^{N}\left(y_i - \sum_{j=1}^{m} x_{ij}\beta_j\right)^2 + \lambda\sum_{j=1}^{m}|\beta_j|$ where y_i is the phenotype of the *ith* individual; x_{ij} is the gene abundance of the *ith* individual at the *jth* gene; β_j is the effect of the *jth* gene; $\sum_{j=1}^{m}|\beta_j|$ is the l1-norm penalty on β, which promotes sparsity in the solution, while $\lambda \geq 0$ is the tuning hyperparameter. The LASSO model was processed through a six-step analytical procedure as follows:

Gene functional annotation was employed to filter out genes with non-functional information, and 151 583 out of 310 192 microbial genes were retained (Supplementary Table S3).

Before applying LASSO, the phenotypic trait corresponding to the treatment group was adjusted by 'sex', applying a logistic regression (link = logit). The residual (adjusted phenotype) was then used in LASSO regression.

Training and test datasets were created with an 80:20 split and using the same initialisation seed (42) as in the mNODE partitions to ensure identical sample assignment across methods. The LASSO model was fitted in the training data set, applying the function 'cv.glment' (Friedman et al., 2010) from the corresponding package in R (R Core Team, 2021) to tune the λ hyperparameter using the cross-validation technique.

After estimating the optimal λ value, the model was trained and optimised again with that value using the 'glment R' function. Finally, only microbial genes with non-zero regression coefficients were considered relevant and thus retained for further analyses.

Results

Phenotypic, behavioural, and cortisol signatures of stress exposure

Phenotypic differences between experimental groups were extensively reported by Clavell-Sansalvador et al. (2024).

Table 1
Summary of mean phenotype, feeding behaviour, and hair cortisol differences between control (n = 30) and chronic social stress (n = 30) groups of pigs.

Trait	Experimental condition		RE	*P*-value
	Control[a]	Stress[b]		
Final BW (kg)	136	127	60.4	<0.0001
Average daily gain (kg)	1.01	0.95	0.003	0.0001
Feed conversion ratio (kg)	2.93	2.87	0.12	0.043
Total number of visits to the feeder	719	589	17.58	<0.0001
Hair cortisol [log(pg/mg)]	3.29	3.42	0.01	<0.0001

Abbreviations: RE = Residual error.
[a] Mean values for the control group.
[b] Mean values for the stress group.

Compared with the control group, the stress group exhibited a decrease in BW, average daily gain, and a marginal difference in feed efficiency (Table 1). Variations in feeding behaviour were noted, with pigs from the stress group visiting the feeder less frequently but spending more time per meal than the control pigs. Notably, cortisol concentrations in hair differed significantly across experimental conditions, with higher levels in the stress group than in the control group (Table 1).

Chronic social stress drives taxonomic and functional remodelling of the pig gut microbiome

Shotgun metagenomics yielded an average of 34 million paired-end reads per sample (SD = 8.1×10^6 reads). After quality control, the taxonomic-based approach quantified the abundance of 513 genera and 1 316 prokaryotic species. Meanwhile, the MAG-based analysis produced 1 087 refined bins, which were dereplicated to remove redundant genomes, yielding 168 MAGs representing 157 species at a 95% ANI threshold (Supplementary Table S4). Based on MIMAG standards (Bowers et al., 2017), 46.87% (75 MAGs) were of high quality, representing near-complete genomes (completeness > 90% and contamination < 5%).

Discriminant analysis revealed that the abundance of 16 MAGs distinguished between experimental conditions with an overall accuracy of 76.39% (Fig. 2A). Half of these MAGs contributed to the classification of the control condition, notably including *Limosilactobacillus* sp002299975 and *Butyrivibrio_A* sp016297265. The other were discriminative of the stress group, with genera such as *Treponema*, *Catenibacterium*, and *Bulleidia* contributing the most (Table 2).

Gene inferences resulted in a total of 310 192 microbial genes. The functional classification provided by DRAM revealed that 48.86% of these genes (151 583) had at least one match against the KOfam, Pfam, or CAZy databases (Supplementary Table S3). To identify microbial functional markers associated with experimental conditions and to reduce feature redundancy, gene-level selection was performed. This approach yielded 64 representative genes (Supplementary Table S5), including eleven genes displaying divergent frequencies between control and stressed pigs and 53 additional genes selected through LASSO regularisation. The resulting gene subset, therefore, captured both experimentally responsive functions and genes with high predictive relevance for group discrimination.

The genus most strongly associated with the control group was *Ligilactobacillus*. Within this group, the most prevalent genes included a *DNA methyltransferase* (K00558) and a *CRISPR-associated endonuclease* (K07012), both of which are involved in genome protection and regulation. In contrast, genes linked to the stress group were predominantly identified in *Escherichia*, *Treponema*, *Blautia*, *Bulleidia*, and *Fimousia*. To be noted, a gene encoding a Rho-binding antiterminator (K19000) identified in *Escherichia* and *Treponema* (Supplementary Table S6) was highly abundant in

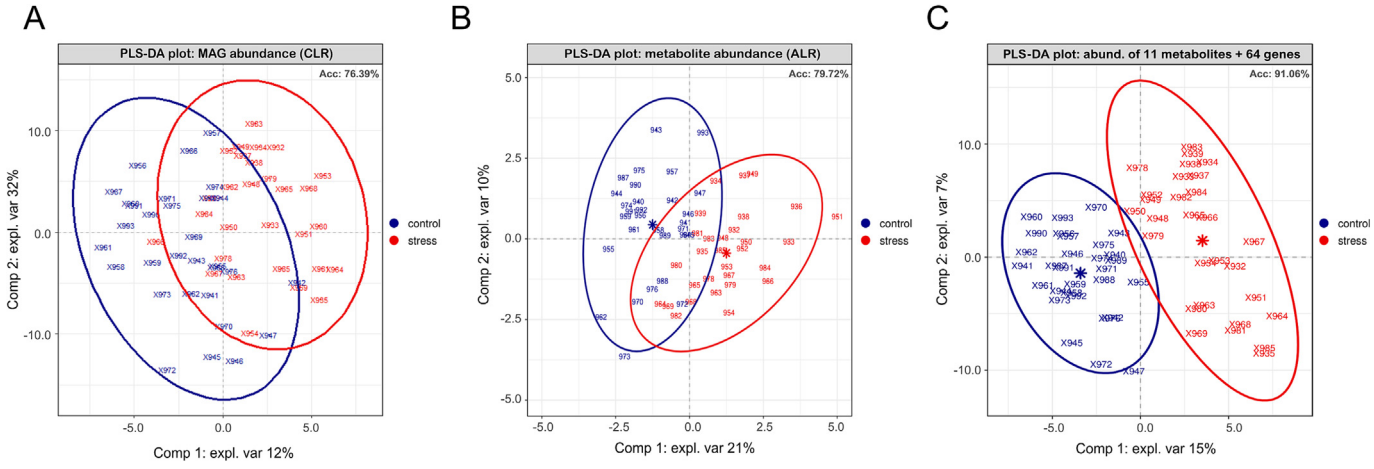

Fig. 2. Faecal sample distribution plots based on PLS-DA of metagenomic, metabolomic and integrative data from control and stress groups of pigs. (A) PLS-DA of CLR-transformed MAG abundance. (B) PLS-DA of ALR-transformed metabolite abundance. (C) PLS-DA after integrating the abundances of eleven discriminant metabolites and 64 selected microbial genes by differential frequency between conditions and by the LASSO machine learning method. Abbreviations: PLS-DA = partial least squares-discriminant analysis; CLR = centred log-ratio; MAG = metagenome-assembled genomes; ALR = additive log-ratio; Acc = accuracy; Comp = component; expl. var. = explained variance.

Table 2
Condition association and loading values of the discriminant Metagenome Assembled Genomes (MAGs) resulting from Partial Least Squares Discriminant Analysis (PLS-DA) using MAG faecal abundance from control and chronic social stress groups of pigs. Features were selected according to a Variable Importance in Projection (VIP) score > 1 from the PLS-DA model.

Code Bin	Taxonomy	Loading value[1]	Condition
bin.989	*Treponema_D* sp018385415	0.44810	Stress
bin.1644	*Treponema_D* sp016293915	0.40803	Stress
bin.474	*Catenibacterium mitsuokai*	0.32005	Stress
bin.667	*Bulleidia* sp900539965	0.25403	Stress
bin.1858	*Treponema_D* sp016294035	0.25068	Stress
bin.2112	*Escherichia coli*	0.24362	Stress
bin.2836	UBA2868 sp004552595	0.12600	Stress
bin.171	*Prevotella* sp004555245	0.08595	Stress
bin.1328	*Treponema_D* sp018385395	−0.04747	Control
bin.370	*Treponema_D* sp016293645	−0.10849	Control
bin.976	*Limimorpha* sp900769945	−0.18245	Control
bin.2627	CAG-964 sp902789345	−0.20109	Control
bin.282	*Methanosphaera* sp022768985	−0.20565	Control
bin.2612	*Butyrivibrio_A* sp016297265	−0.23054	Control
bin.1187	F23-B02 sp004556755	−0.23879	Control
bin.2285	*Limosilactobacillus* sp002299975	−0.28299	Control

[1] Loading values represent the contribution (weight) of each MAG to the latent components that maximise the separation between the sample groups in the PLS-DA.

pigs under the stress condition, suggesting altered transcriptional regulation.

Among the genes selected by LASSO, *Blautia* contributed genes involved in catabolic processes, such as *beta-galactosidase* (K12308) and *gamma-glutamylcyclotransferase* (K00682)—as well as in bacterial signalling, including a *sensor histidine kinase* (K07718). Additional stress-associated functions included oxidative stress defence enzymes, notably a thioredoxin-dependent peroxiredoxin (K03564) identified in *Bulleidia*, along with multiple transcriptional regulators and two-component sensory systems, indicating enhanced microbial responsiveness to environmental stress. Genes involved in horizontal gene transfer and genome plasticity, such as integrases, transposases, reverse transcriptase, and phage-related recombination proteins, were also relevant. Altogether, we suggest functional shifts that support microbial survival and metabolic flexibility under stress conditions.

Faecal metabolic fingerprint of chronic stress

Through rigorous analysis of the reverse-phase liquid chromatography–quadrupole time-of-flight mass spectrometry spectra and extensive database searching (see Methods), 26 195 peaks were detected, of which 426 had corresponding MS/MS spectra. After filtering, 114 tentative metabolites with a total annotation score ≥ 70% were successfully identified and retained for further analysis. Notably, a biological replicate was included as an external quality control, showing a Pearson's correlation coefficient of 0.98, thereby indicating a high degree of similarity and strong technical reproducibility (see Supplementary Figure S1).

Metabolite-based discriminant analysis reveals gut-brain axis-related biomarkers

PLS-DA showed that, based on VIP scores, 11 of the 114 metabolites could discriminate the stress group from the control, with an accuracy of 79.72%, sensitivity of 78.48%, and specificity of 80.96% (Fig. 2B). Among them, four tentative metabolites, serotonin, sinapine, elaidic acid, and 2-acetamidophenol (**AAP**), were distinctive indicators of the control group, while the other seven were indicators of the stress group (Table 3).

Statistical associations between metabolites, hair cortisol levels, and the abundance of selected microbial genes were also explored. A significant correlation ($p < 0.05$) was observed between two of the eleven metabolites and the hair cortisol levels. This included a positive correlation with the putative indicator of stress n-octadecylamine (r = 0.37, $p = 5.25 \times 10^{-3}$) and a negative correlation with the neurotransmitter serotonin (r = –0.32, $p = 0.01$; Fig. 3).

Microbiome–metabolite interaction networks indicate adaptive metabolic regulation under stress

Correlation analyses further explore associations between discriminant metabolites and microbial taxa. Positive correlations were also observed between the control-discriminant metabolite AAP and several butyrate-producing genera (Fig. 4), including *Roseburia* (r = 0.24), *Butyrivibrio* (r = 0.28), *Coprococcus* (r = 0.20), and *Anaerobutyricum* (r = 0.18), as well as with lesser-documented taxa, such as *PeH17* (r = 0.45) and *Sodaliphilus* (r = 0.36). Conversely, the stress-discriminant metabolite N-α-acetyl-L-lysine showed unexpected positive correlations with *Lactobacillus* (r = 0.56) and *Limosilactobacillus* (r = 0.42). To further investigate the microbial origin of these metabolites, *in silico* exploratory analyses were conducted using the MicrobeMASST database. Nine of the eleven discriminant metabolites had matches in MicrobeMASST (Supplementary Table S7). In particular, the mass spectrum of AAP matched metabolites detected in *Bifidobacterium longum* isolates and other prevalent intestinal species, including *Enterococcus faecalis*.

At the gene level, microbial genes that exhibited a positive association with the abundance of the stress-discriminant metabolite xanthosine consistently belonged to stress-associated species, including *Prevotella pectinovora*, *Blautia* sp., and *Holdemanella porci* (Supplementary Table S8, Fig. 4). By contrast, genes exhibiting a negative links with xanthosine were identified in commensal or health-associated species, including *Limimorpha* sp., *Butyrivibrio* sp., *Ruminococcus flavefaciens*, *Anaerobutyricum hallii*, and *Clostridium* sp (Supplementary Table S8, Fig. 4), and interestingly, they were positively associated with AAP (Supplementary Table S9). These genes were mainly annotated as transposases and ribosomal subunits.

Finally, focusing on control indicators, to disentangle potential gene-to-gene interactions in serotonin metabolism, abundance associations between selected microbial genes and genes involved in serotonin-related pathways were examined. The genome of *Prevotella* carried the threonine aldolase gene (K01620) selected by LASSO, which showed a positive association with the *Fimousia* and *Treponema* genes *3-deoxy-7-phosphoheptulonate synthase* (r = 0.96; r = 0.91) and *tryptophan* synthase *alpha chain* (r = 0.94; r = 0.89), both of which are commonly linked to serotonin abundance. Likewise, the *large subunit ribosomal protein L23* gene (K02892), also selected by LASSO, found in the genome of *Ruminococcus*, was positive and strongly correlated with the *tryptophan synthase α-chain* (r = 0.94), *tryptophanase* (r = 0.97), and *3-deoxy-7-phosphoheptulonate (DAHP) synthase* (r = 0.97) genes of *Escherichia*.

Microbiome-metabolome integrative analyses enhance chronic stress detection in pigs

A final PLS-DA model was performed by integrating microbiome data from the 64 selected genes with the abundance profiles of the 11 discriminant metabolites. For comparison, discriminant analysis using only the 64 selected genes achieved an accuracy of 87% (Supplementary Figure S2). The integrative approach combining microbial gene and metabolite information substantially improved

Table 3
Description of the eleven tentatively identified metabolites discriminating stress and control pigs based on untargeted reverse-phase liquid chromatography quadrupole time of flight mass spectrometry (RP-HPLC-Q/TOF-MS/MS) metabolomics and the subsequent Partial Least Squares Discriminant Analysis (PLS-DA) analysis. Features were selected according to a Variable Importance in Projection (VIP) score > 1 from the PLS-DA model. Metabolites were annotated following the Metabolomics Standards Initiative guidelines at level 2a, based on accurate precursor *m/z* and MS/MS spectral library matching using MS-DIAL software v. 4.9.221218. The table reports the compound name, molecular formula, observed mass-to-charge ratio (*m/z*), detected adducts (positive ionisation mode), chromatographic retention time (Rt, min), PLS-DA loading values and the associated condition.

Compound name	Molecular formula	*m/z*	Adduct[1]	Rt (min)	Loading value[2]	Condition
Serotonin	$C^{10}H_{12}N_2O$	177.1023	$[M+H]^+$	2.232	0.3892	Control
Sinapine	$C_{16}H_{24}NO_5$	251.0920; 207.0658; 179.0709; 147.0438; 119.0487	$[Cat\text{-}C_3H_9N]^+$; $[Cat\text{-}C_5H_{13}NO]^+$; $[Cat\text{-}C_6H_{13}NO_2]^+$; $[Cat\text{-}C_7H_{17}NO_3]^+$; $[Cat\text{-}C_8H_{17}NO_4]^+$	4.210	0.3575	Control
2-acetamidophenol	$C_8H_9NO_2$	152.0707; 110.0606	$[M+H]^+$; $[M+H\text{-}C_2H_2O]^+$	3.362	0.2571	Control
Elaidic acid	$C_{18}H_{34}O_2$	283.2647	$[M+H]^+$	10.089	0.1288	Control
Uracil	$C_4H_4N_2O_2$	113.0373	$[M+H]^+$	0.819	–0.1814	Stress
Xanthosine	$C_{10}H_{12}N_4O_6$	153.0389	$[M+H\text{-}C_5H_8O_4]^+$	2.089	–0.2443	Stress
Thymine	$C_5H_6N_2O_2$	127.0404	$[M+H]^+$	1.569	–0.2475	Stress
N-α-acetyl-L-lysine	$C_8H_{16}N_2O_3$	189.1232	$[M+H]^+$	0.605	–0.2594	Stress
6-(6-aminohexanamido) hexanoic acid	$C_{12}H_{24}N_2O_3$	245.186	$[M+H]^+$	2.661	–0.2843	Stress
L-β-homolysine	$C_7H_{16}N_2O_2$	144.1029	$[M+H\text{-}NH3]^+$	0.942	–0.3065	Stress
n-octadecylamine	$C_{18}H_{39}N$	270.3159	$[M+H]^+$	9.891	–0.4921	Stress

Abbreviations: *m/z* = Mass-to-charge ratio; Rt = Retention time; PLS-DA = partial least squares discriminant analysis.
[1] Protonated molecules are represented as $[M+H]^+$.
[2] Loading values represent the contribution (weight) of each metabolite to the latent components that maximise the separation between the sample groups in the PLS-DA.

discrimination between experimental groups, increasing classification accuracy from 79.72% (metabolites alone) and 87% (microbial genes alone) to 91.06%, with sensitivity and specificity reaching 90.25% and 91.87%, respectively. This is illustrated by the PLS-DA sample distribution plots, where condition-specific functional profiles (Fig. 2C) separate samples more clearly than taxonomic shifts (Fig. 2A).

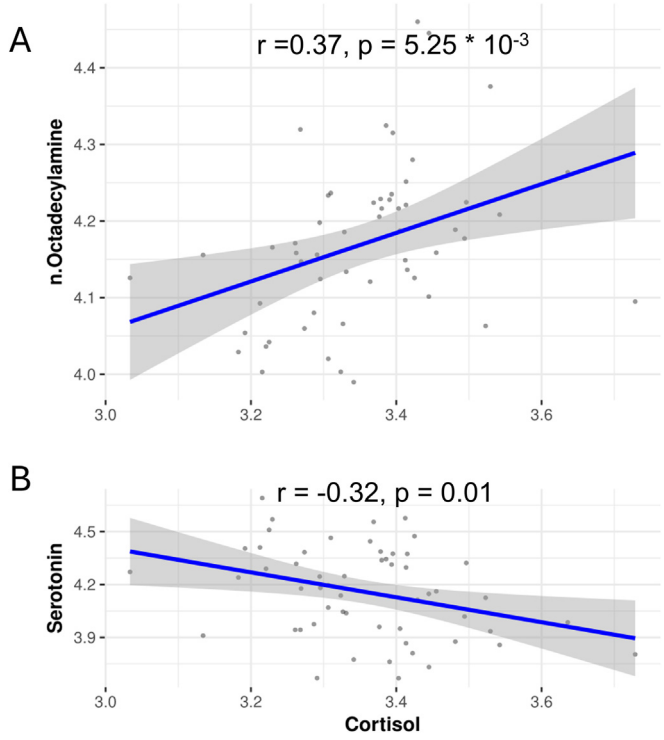

Fig. 3. Correlation patterns of hair cortisol levels with the abundance of two major condition-discriminant metabolites (stress vs control) in pigs. The scatter plot reveals correlations between hair cortisol concentrations and the selected metabolites by PLS-DA (VIP > 1): (A) stress-discriminant n-octadecylamine and (B) control-discriminant serotonin. Pearson's correlation coefficients (r) and associated *p*-values are shown. A significant positive correlation was observed for n-octadecylamine (r = 0.37, $p = 5.25 \times 10^{-3}$), whereas serotonin showed a significant negative correlation (r = –0.32, $p = 0.01$). Abbreviations: PLS-DA = partial least squares-discriminant analysis; VIP = variable importance in projection.

Microbial gene resolution improves prediction of the neurotransmitter serotonin

Microbiome-metabolite interactions were predicted using four complementary layers of microbial information, ranging from genus to gene repertoire. Fig. 5 displays the accuracy of the prediction of the eleven discriminant metabolites using microbial information. Prediction performance varied with the level of microbial resolution employed. At the genus level, correlations between observed and predicted metabolite levels ranged from 0.05 to 0.91 (mean r = 0.69). In this case, serotonin showed the lowest prediction accuracy (r = 0.05), whereas AAP (r = 0.90) and elaidic acid (r = 0.91) were the best-predicted metabolites. These two compounds consistently exhibited the highest predictive accuracy across all four metagenomic profiles (Fig. 5). Species-level predictions followed a similar trend but showed lower overall performance (mean r = 0.47), mainly due to reduced prediction accuracy for six of the eleven metabolites, while the remaining five showed comparable performance to genus-level predictions.

Predictions based on MAG abundance yielded correlations ranging from 0.18 to 0.86 (mean r = 0.43), improving the prediction accuracy of serotonin and uracil (Fig. 5) but decreasing the prediction values for L-β-homolysine, Nα-acetyl-L-lysine, and xanthosine. At the functional level, predictions based on the abundance of the 64 selected microbial genes reported from null to high (r = 0.79) prediction ability (mean r = 0.51). Even though other metabolites were not better predicted by microbial gene profiles, an improvement was observed in the case of serotonin (r = 0.74), L-β-homolysine (r = 0.51) and xanthosine (r = 0.65; Fig. 5). These results suggest that microbial gene profiles may better capture metabolic interactions involving these compounds, particularly the control-discriminant neurotransmitter serotonin.

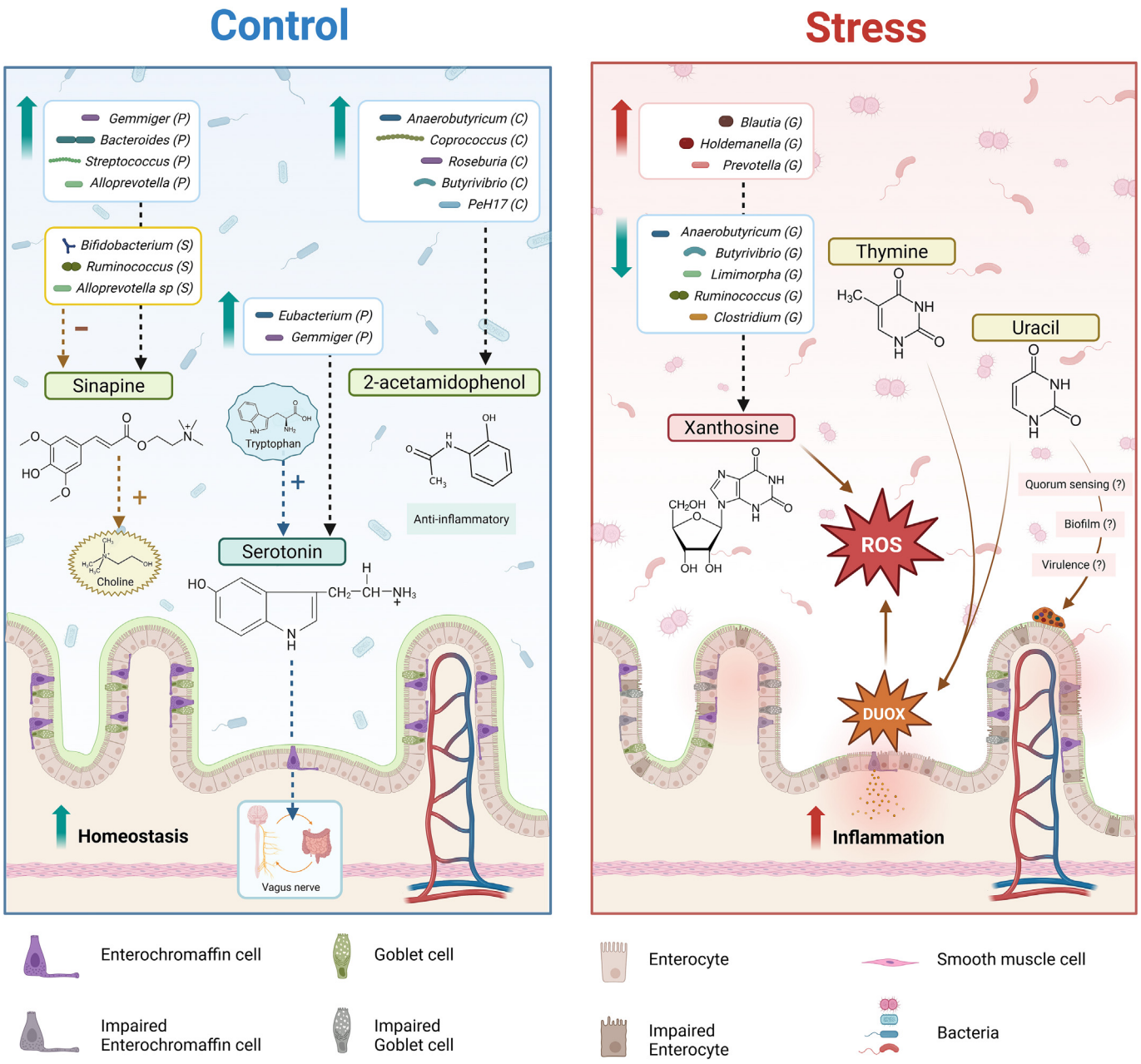

Fig. 4. Summary of the mNODE and the correlation analyses results reflecting the patterns of the pig gut microbiome and metabolite biomarkers under control and stress conditions. In the control group (left panel), microbial taxa in green (P and C) potentially promote higher levels of beneficial metabolites, including serotonin, sinapine, and AAP, contributing to homeostasis. The potential consumption of sinapine, which also possesses antioxidant properties, by some bacteria (S), in yellow (e.g. *Bifidobacterium*), could produce choline, while AAP has anti-inflammatory effects, and serotonin acts as a neurotransmitter, supporting gut-brain communication. In the stressed group (right panel), increased levels of pyrimidine bases such as uracil and thymine were observed, which are reported to potentially trigger the activation of the enterocyte DUOX. Furthermore, the gene abundance (G) of *Blautia*, *Holdemanella,* and *Prevotella* correlates positively with increased xanthosine levels, while the gene abundance of *Anaerobutyricum*, *Butyrivibrio*, *Limimorpha*, *Ruminococcus,* and *Clostridium* correlates negatively. Scientific literature associates these metabolites with the generation of ROS, the induction of oxidative stress and the subsequent inflammation in the gut. Additionally, uracil may activate *quorum sensing*, biofilm formation, and virulence factors, exacerbating gut dysbiosis and promoting inflammatory responses. Created in BioRender (https://BioRender.com/l29x60). Abbreviations: mNODE = machine learning method based on neural ordinary differential equations; *P* = predicted positive associations by the mNODE method; C = positive Pearson's correlations based on genus abundance; AAP = 2-acetamidophenol; S = negative susceptibility mNODE association; DUOX = dual oxidase; G = positive Pearson's correlations based on microbial gene abundance; ROS = reactive oxygen species.

Susceptibility modelling based on neural ordinary differential equations reveals microbial contributions to gut metabolic dynamics

mNODE susceptibility analysis revealed distinct interaction patterns among key metabolites under control and stress conditions. Notably, MAGs with predicted positive susceptibility to serotonin, such as *Gemmiger* (r = 0.25) and *Eubacterium* Q (r = 0.11; Fig. 4), carried the gene encoding tryptophan synthase subunit A, which participates with tryptophan synthase subunit

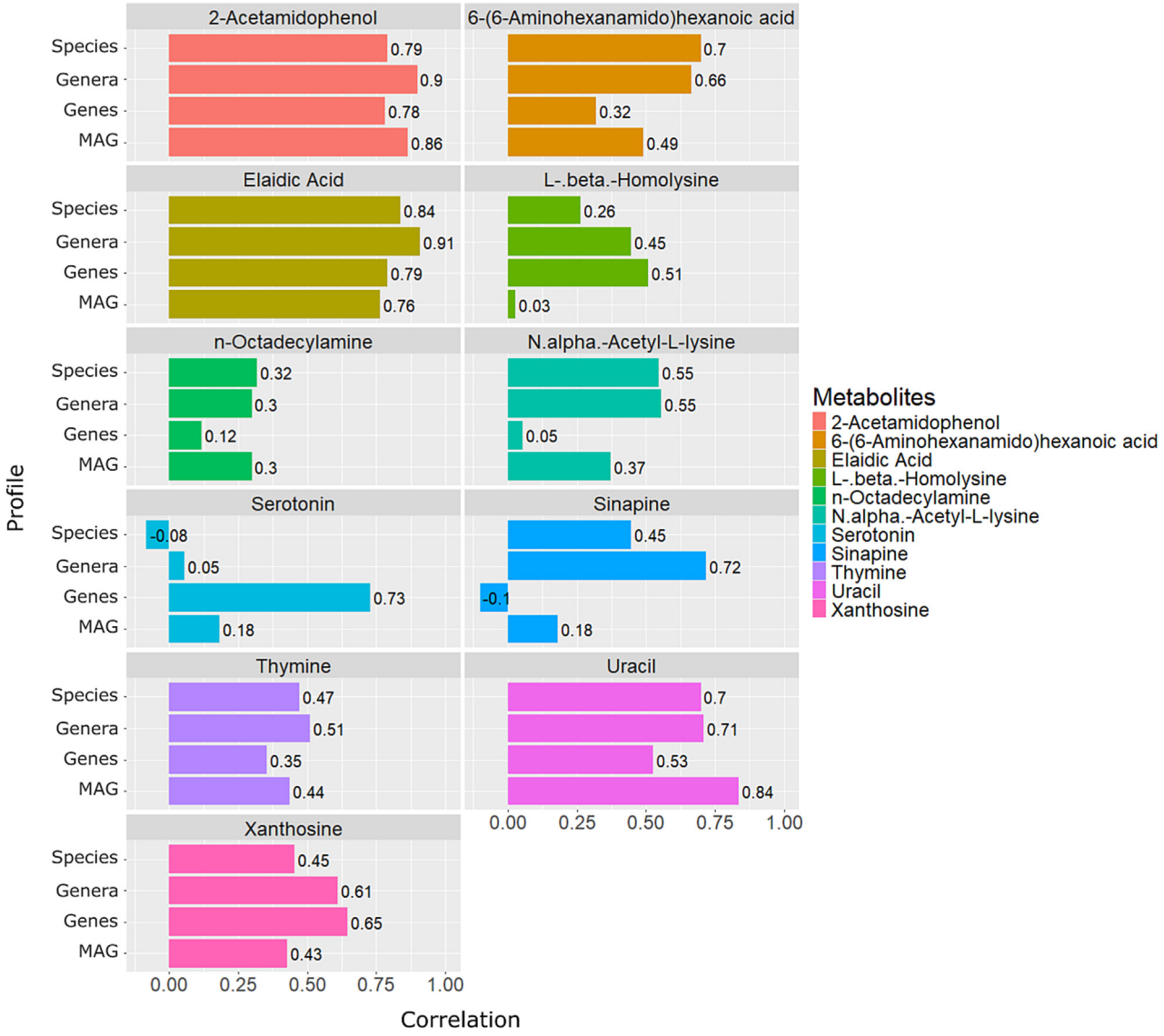

Fig. 5. Metabolite prediction from pig faecal samples using the metabolomic profile predictor based on mNODE. The figure displays the correlation between predicted and observed abundances of the eleven discriminant metabolites identified by PLS-DA, as obtained from the mNODE model trained on microbial profiles at four taxonomic and functional levels. Microbial abundance tables derived from metagenomic data included species (n = 1 316), genus (n = 513), gene (n = 64), and MAG (n = 168) levels. For the microbial gene profiles, due to the large number of variables (310 192 genes), frequency-based filtering and LASSO feature selection were applied before modelling. Abbreviations: mNODE = machine learning method based on neural ordinary differential equations; PLS-DA = partial least squares-discriminant analysis; MAG = metagenome-assembled genome.

B in the tryptophan synthase complex to convert indole and serine to tryptophan, a precursor for serotonin. In contrast, at the gene level, serotonin and xanthosine, a stress-discriminant metabolite, exhibited an opposing pattern of microbial susceptibility (Fig. 6), supporting the existence of divergent microbiome-metabolite interaction networks between control and stress conditions.

In addition, subtle negative susceptibility values, suggesting potential aggregated contribution to sinapine consumption, were also observed for several bacterial species, including *Bifidobacterium thermacidophilum* (r = –0.02), *R. flavefaciens* (r = –0.02), *Bifidobacterium boum* (r = –0.03), *Alloprevotella* sp. (r = –0.02), and *Treponema* sp (r = –0.03; Fig. 4). Conversely, mNODE predictions also showed positive but weak associations of sinapine with *Gemmiger qucibialis* (r = 0.03), *Bacteroides_F* sp. (r = 0.03), *Streptococcus faecavium* (r = 0.03), *Streptococcus hyointestinalis* (r = 0.03), and *Alloprevotella* sp (r = 0.02).

Similarly, the mNODE model at both MAG and genus levels identified weak but consistent associations between elaidic acid, a trans isomer of oleic acid and a common dietary *trans*-fatty acid, and specific microbial taxa. Positive predictions were observed with *Eubacterium* (r = 0.05 at both levels), whereas negative associations were detected with *Bruticola* (r = –0.06; r = –0.07), *Akkermansia* (r = –0.15; r = –0.06), and *Fimousia* (r = –0.06; r = –0.04). Although individual susceptibility values were modest, elaidic acid, together with AAP, appears to be a reliable control-group indicator, reflecting coordinated contributions from multiple microbial taxa. This is further supported by its consistently high predictive accuracy across microbiome datasets, decreasing from the genus level (r = 0.91) to the gene level (r = 0.79; Fig. 5).

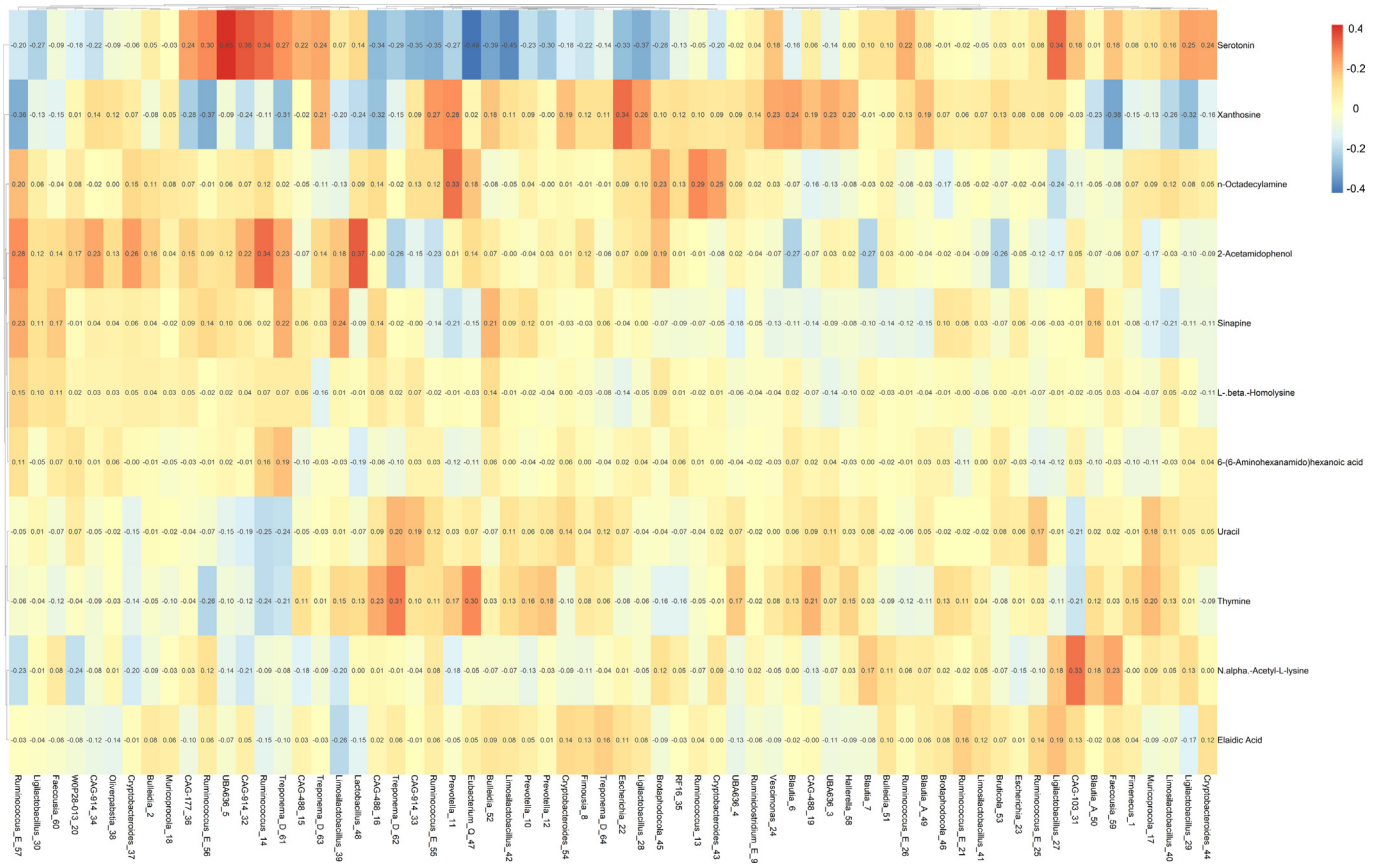

Fig. 6. Gene-level susceptibility heatmap of the eleven tentatively identified discriminant metabolites in pigs based on mNODE. Rows represent metabolites and columns represent microbial genes annotated with their corresponding taxonomy. Positive susceptibility values (>0) are shown in red, suggesting potential production of the metabolite or direct or indirect involvement in its anabolism, whereas negative values (<0) are shown in blue, indicating potential consumption or inhibition of metabolite production. Opposing susceptibility patterns are observed for metabolites such as serotonin and xanthosine, supporting their roles as indicators of control and stress conditions, respectively. Abbreviations: mNODE = machine learning method based on neural ordinary differential equations.

Discussion

This study integrated shotgun metagenomics with untargeted faecal metabolomics in a porcine model of prolonged social stress. Stress induced notable shifts in the faecal metabolome and gut microbiome composition. These changes, along with differences in hair cortisol and previously reported alterations in performance and microbiota (Clavell-Sansalvador et al., 2024), highlight the profound impact of prolonged stress on both host physiology and the gut microbial ecosystem. Our approach further enables the exploration of microbiome-metabolite interactions as potential non-invasive biomarkers of stress.

We further evaluated how precisely the eleven discriminative metabolites could be predicted from metagenomic data at different microbial resolutions. In agreement with the original mNODE study (Wang et al., 2023a), prediction accuracy varied by metabolite. Incorporating microbial genes associated with the experimental conditions improved discrimination, showing that functional profiles provide complementary mechanistic insight. From an applied perspective, this approach supports the development of a reduced biomarker panel, measurable via targeted methods like qPCR or metabolomic quantification, reducing the need for full metagenomic and metabolomic profiling. This strategy lowers costs, computational demand, and processing time, enabling scalable stress monitoring in livestock.

Control-discriminant metabolites, such as AAP, exhibited a positive trend in compound bioactivity. Even though its biosynthesis is not yet fully understood, AAP, known for its anti-inflammatory (Siddiqui et al., 2019) and anti-arthritic (Perveen et al., 2014; Gul et al., 2017) properties, has been reported to be naturally produced by bacteria with broad secondary metabolism (Guo et al., 2020). Its abundance correlated with butyrate-producing genera like *Coprococcus* and *Anaerobutyricum*, previously identified as indicators of healthy pigs (Clavell-Sansalvador et al., 2024). This supports AAP as a marker of favourable gut conditions, further strengthened by its high predictability from metagenomic profiles. This highlights its potential as a practical indicator of porcine welfare and gut health. Faecal serotonin levels were also associated with non- or low-stress conditions. Serotonin is a key signalling molecule that regulates mood, cognition, circadian rhythms, and digestive function (Kaczmarek et al., 2017; Jiang et al., 2024). Although more than 90% of serotonin is produced by enterochromaffin cells (Xie et al., 2020), the gut microbiota— especially spore-forming bacteria (Yano et al., 2015)—modulate its activity through short-chain fatty acids and bile-acid signalling (Martin et al., 2017). Furthermore, bacterial biosynthesis of serotonin has been confirmed across several genera, including *Escherichia*, *Enterococcus*, *Bacillus, Lactobacillus, Ligilactobacillus and Limosilactobacillus* (Strandwitz, 2018; Wang et al., 2023b; Moretti et al., 2025), with *Lactobacillus* particularly linked to gut serotonin in pigs (Liu et al., 2023). Microbial gene-based profiling better predicted serotonin abundance, and MAGs with predicted positive susceptibility for this metabolite harboured key enzymes for involving serotonin precursors, underscoring the importance of species carrying relevant biosynthetic genes.

Intriguingly, gene-level correlations revealed strong links between genes from different species not directly involved in sero-

tonin metabolism, such as the *ribosomal protein L23* in *Ruminococcus* and the *threonine aldolase* in *Prevotella*. Interactions between these genes and tryptophan metabolism-related genes of *Escherichia, Fimousia* and *Treponema* may enable these bacteria to adjust their ribosomal machinery in response to increased levels of serotonin precursors. This suggests an indirect role in serotonin anabolism, likely mediated by threonine-to-glycine metabolism, with glycine acting as an inhibitory neurotransmitter complementing serotonin's effects. Although host-derived serotonin predominates, these interspecific interactions may contribute to the coordinated regulation of amino acid metabolism, thereby influencing serotonin gut levels and its downstream effects on gut-brain communication. Importantly, all pigs received comparable dietary tryptophan (0.30–0.43%), indicating that faecal serotonin differences likely reflect management-induced stress rather than diet. Consistently, discriminant analysis identified serotonin, whether produced by the host or bacteria, as a control-associated metabolite. Future studies using metaproteomics or microbial gene expression could clarify the microbiota's contribution.

Similarly, although both experimental groups were fed the same standard diet, sinapine, a major phenolic component of *Brassicaceae* seeds (Mittasch et al., 2010) was identified as a non- or low-stress indicator. Like AAP, sinapine exhibits anti-inflammatory (Liu et al., 2020) and antioxidant (Li et al., 2022) properties and can influence host metabolism via choline-derived trimethylamine N-oxide (Chen et al., 2019). In mice, sinapine administration reduces non-alcoholic fatty liver disease progression by modulating the gut microbiota (Li et al., 2019), decreasing the Firmicutes/Bacteroidetes ratios and increasing the abundance of beneficial probiotics like *Lactobacillus* and Bifidobacterium. Moreover, they reported negative associations of this metabolite with *Erysipelotrichaceae*, which in turn are indicators of social stress in pigs (Clavell-Sansalvador et al., 2024). Sinapine-degrading bacteria have been identified within the intestinal microbiota of laying hens (Yu et al., 2016), but natural microbial producers have not been described. While AAP was consistently predicted across all levels and its microbial origin is well-supported in the literature, evidence for sinapine is weak. Therefore, rather than being considered a microbial metabolite, we propose that future studies investigate sinapine's potential role as a prebiotic.

Xanthosine, thymine, uracil, n-octadecylamine, and N-α-acetyl-L-lysine were identified as stress-associated faecal metabolites. Xanthosine, a purine derivative, contributes to reactive oxygen species generation through xanthine and uric acid metabolism (Bortolotti et al., 2021). Reactive oxygen species play essential roles as signalling molecules and in immune defence, but their excessive accumulation can lead to tissue damage and organ dysfunction and contribute to tumour development (Yang and Lian, 2020; Cheung and Vousden, 2022). In line with our previous research (Clavell-Sansalvador et al., 2024), genes linked to high xanthosine abundance were found in stress-associated species like *D. longicatena* and *H. porci*, whereas beneficial species, such as *Butyrivibrio* sp., *R. flavefaciens* or *A. hallii* were negatively associated. Supporting this, reductions in xanthine, followed by increases in indoles and serotonin, have been reported in responders with major depressive disorder compared to non-responders treated with citalopram (Bhattacharyya et al., 2019). In this study, serotonin and xanthosine showed opposing roles as metabolomic indicators, with stronger predictions at the gene level but divergent microbial susceptibility patterns at that resolution. This is intriguing and may also suggest that genes with high predictive value for xanthosine could have an inverse metabolic relationship and indirectly influence faecal serotonin levels. A similar trend was observed for AAP, as genes negatively associated with xanthosine, mainly transposases and ribosomal subunits, showed positive associations with this metabolite.

Among the stress indicators, the pyrimidine bases thymine and uracil, along with elevated xanthosine levels, may contribute to gut inflammation through increased reactive oxygen species potential and their involvement in bacterial *quorum-sensing*, biofilm formation, and virulence regulation (Ueda et al., 2009). *Quorum-sensing* pathways are vital for bacterial communication and the coordination of virulence factor expression, potentially escalating pathogenicity under stress conditions. Uracil, produced by pathogenic bacteria, can act as a ligand to initiate cascade-like signalling in enterocytes that activates host dual oxidase to produce reactive oxygen species (Lee et al., 2013, 2015, 2018; Ha et al., 2009). Kim et al. (2020) showed that pathogens produce uracil and ribose from gut-luminal uridine, triggering host defences, interbacterial communication, and pathogenesis in *Drosophila*. Genes mediating nucleotide metabolism, more common in pathogens than in commensal bacteria, modulate these processes, including Rho-dependent transcription termination (K19000), which varied significantly between stressed and control pigs in genomes of the opportunistic *Treponema*, a genus recently reported as a stress indicator in growing pigs (Clavell-Sansalvador et al., 2024; Nguyen et al., 2023).

Interestingly, n-octadecylamine was positively correlated with hair cortisol, though its role in stress responses and cortisol regulation remains unclear and requires further investigation. N-α-acetyl-L-lysine, an acetylated lysine derivative that primarily arises from post-translational protein modification, also indicated stress. Surprisingly, it was positively correlated with the health-associated genera *Lactobacillus* and *Limosilactobacillus*, in line with previous reports (Peng et al., 2023). Lysine acetylation can influence the biological functions of lysine residues within proteins, altering processes such as gene regulation or protein interaction (Christensen et al., 2019; Hao et al., 2024). As an essential limiting amino acid in human and pig diets, long-term lysine restriction affects cell proliferation, metabolism, and potentially gut microbiota and AMPK signalling (Yin et al., 2018).

Based on our findings, we propose that monitoring xanthosine, thymine, uracil, n-octadecylamine, and N-α-acetyl-L-lysine levels could provide valuable insights into the stress status and its effects on porcine gut health. However, it should be noted that the prediction reliability for some of them, such as thymine abundance, was consistently moderate across all employed microbial levels. This outcome was not unexpected, given that thymine is a ubiquitous pyrimidine base. Its widespread presence may contribute to the lower predictability of its abundance based on the metagenomic profile alone, as it is not uniquely associated with specific taxa or conditions. In contrast, uracil abundance demonstrated higher predictive accuracy. This increased reliability may be attributable to uracil's more specific role and its association with bacterial processes, such as *quorum-sensing* and stress response mechanisms, which may be less widely distributed than those involving thymine.

As previously mentioned, not all metabolites were predicted with equal accuracy. Aside from AAP and elaidic acid, there was no single, high-precision source of information for accurate prediction across all microbial levels. This observation underscores the need to interpret metabolomic predictions derived from partial metagenomic information carefully. Moreover, as noted by Wang et al. (2023a), the accuracy of mNODE predictions can be impacted in metabolites when production interactions overlap with consumption at the microbiome level (i.e., the same taxa produce and consume a target metabolite). Similarly, it is plausible that metabolites originating solely from microbial metabolism can be more accurately predicted based on microbial composition than

molecules derived from host or dietary metabolism. This is because microbial metabolites may have a more direct and consistent relationship with specific microbial taxa. However, distinguishing microbial metabolites from those of host or dietary origin is challenging because of the complex interplay and overlap among these metabolic pathways. Consequently, further research is essential to better disentangle these sources and understand their specific contributions. Remarkably, predictions based on MAGs did not necessarily achieve higher accuracy than genus- or species-based profiles. Similar results have recently been reported in metabolomic prediction from metagenomes (Majzoub et al., 2024). This may reflect the limited species coverage in MAG collections compared to the broader diversity captured by taxonomic profiling. Therefore, combining metagenomic and taxonomic approaches offers complementary strengths with lower computational requirements, making it suitable for shallow shotgun sequencing experiments.

Despite these constraints, our study offers new insights into microbiome-metabolite interactions under prolonged social stress, contributing to a deeper understanding of how stress influences microbial ecosystems and their metabolic outputs. This includes the prediction of relevant metabolites from metagenomic data and the identification of putative non-invasive faecal biomarkers of welfare. Our comprehensive approach highlights the utility of the porcine model in bridging the gap between microbial ecology and host metabolic responses to stress. The notable parallels between our results and reported alterations in the human metabolome and gut microbiome under stress further support their translational value for gut-brain axis research. Future studies should explore multiple pig breeds, different stressors, and longitudinal sampling to validate these microbial shifts and refine biomarker identification.

Conclusions

This study highlights the effectiveness of integrating metagenomic and untargeted metabolomic data to identify candidate non-invasive biomarkers of welfare and prolonged stress-related conditions in pigs. Combining discriminant metabolites and microbial genes significantly improved the sample discriminant accuracy, revealing distinct microbial and metabolic shifts between the control and stressed groups. The study identified serotonin and anti-inflammatory metabolites, such as AAP and sinapine, as indicators of the control group, whereas xanthosine, pyrimidine bases, n-octadecylamine and stress-related microbial genes were identified as stress indicators. Additionally, the integrative approach employed in this study provides new insights into putative interspecific interactions modulating microbiome-metabolite signatures of prolonged stress. These findings underscore the value of the porcine model in advancing our understanding of the microbiome-gut-brain axis and hold promise for enhancing both animal welfare and human health interventions.

Supplementary material

Supplementary Material for this article (https://doi.org/10.1016/j.animal.2026.101823) can be found at the foot of the online page, in the Appendix section.

Ethics approval

All animal experiments described in the present study were conducted at the IRTA Experimental Farm in Monells in accordance with European Union directive 2010/63/EU and authorised by the Institutional Ethics Committee of IRTA (protocol code 10329).

Data and model availability statement

The raw sequencing data employed in this study have been submitted to the NCBI's Sequence Read Archive (https://www.ncbi.nlm.nih.gov/sra) and BioProject under accession number: PRJNA1208715. Microbial gene functional annotation data are available in the Supplementary Table S3. The metabolomic data are available upon request and not publicly available because they are part of ongoing analyses.

The bioinformatic pipeline used in this study is publicly accessible at: https://github.com/Yuliaxis/MetaG_MetaB.

Declaration of generative AI and AI-assisted technologies in the writing process

The authors did not use any artificial intelligence-assisted technologies in the writing process, except for those employed to improve the grammar of certain sentences.

Author ORCIDs

R. Río-López: https://orcid.org/0009-0000-6699-6486.
I.-T. Vourlaki: https://orcid.org/0000-0002-3381-5287.
A. Clavell-Sansalvador: https://orcid.org/0000-0003-1217-2216.
A. Valdés: https://orcid.org/0000-0002-7901-5816.
L. Padilla: https://orcid.org/0000-0001-6639-6915.
L. J. García-Gil: https://orcid.org/0000-0002-5064-8361.
X. Xifró: https://orcid.org/0000-0002-7417-9475.
M. Ballester: https://orcid.org/0000-0002-5413-4640.
R. Quintanilla: https://orcid.org/0000-0003-3274-3434.
J. Ochoteco-Asensio: https://orcid.org/0000-0003-2704-3986.
F. X. Prenafeta-Boldú: https://orcid.org/0000-0001-9514-7029.
A. Dalmau: https://orcid.org/0000-0003-2248-6796.
Y. Ramayo-Caldas: https://orcid.org/0000-0002-8142-0159.

CRediT authorship contribution statement

R. Río-López: Writing – review & editing, Writing – original draft, Formal analysis, Data curation. **I.-T. Vourlaki:** Writing – review & editing, Writing – original draft, Formal analysis, Data curation. **A. Clavell-Sansalvador:** Writing – review & editing, Writing – original draft. **A. Valdés:** Writing – review & editing, Writing – original draft, Methodology, Formal analysis, Data curation. **L. Padilla:** Writing – review & editing, Writing – original draft. **L.J. García-Gil:** Writing – review & editing. **X. Xifró:** Writing – review & editing. **M. Ballester:** Writing – review & editing. **R. Quintanilla:** Writing – review & editing. **J. Ochoteco-Asensio:** Writing – review & editing. **F.X. Prenafeta-Boldú:** Writing – review & editing. **A. Dalmau:** Writing – review & editing, Writing – original draft, Supervision, Project administration, Funding acquisition, Data curation, Conceptualisation. **Y. Ramayo-Caldas:** Writing – review & editing, Writing – original draft, Supervision, Project administration, Methodology, Investigation, Funding acquisition, Formal analysis, Data curation, Conceptualisation.

Declaration of interest

The authors declare no competing interests.

Acknowledgements

We thank Olga González-Rodríguez, Gustavo Zigovski, and Leandro. B. Costa for their valuable contributions during sample

collection and for providing feedback on the manuscript. The pigs that participated in this study and their caretakers from Monells, IRTA, are acknowledged. Figs. 1 and 4 were created with BioRender.com. This work was carried out within the framework of the doctoral programme in Microbiology at the Autonomous University of Barcelona (UAB), Barcelona, Spain.

Financial support statement

This research was financially supported by PID2021-126555OB-I00 project funded by MCIN/AEI/10.13039/501100011033, 'ERDF A way of making Europe'. RRL was funded by AGAUR-FI 'Joan Oró' grant (2024 FI-1 00034) awarded by the Department of Research and Universities of the Government of Catalonia and co-financed by the European Social Fund Plus (ESF+). ITV was funded by the HoloRuminant (101000213) H2020 projects. ACS was funded with a PhD fellowship (PRE2022-101829) awarded by the Spanish Ministry of Education and Culture. YRC received the 'Ramon y Cajal' grant (RYC2019-027244-I) funded by MCIN/AEI/ https://doi.org/10.13039/501100011033 and by 'ESF Investing in your future'.

References

Alberdi, A., 2022. distillR: R package for distilling functional annotations of bacterial genomes and metagenomes. Github. Retrieved on 8 October 2024 from: https://github.com/anttonalberdi/distillR.

Amin, N., Liu, J., Bonnechere, B., MahmoudianDehkordi, S., Arnold, M., Batra, R., Chiou, Y.-J., Fernandes, M., Ikram, M.A., Kraaij, R., Krumsiek, J., Newby, D., Nho, K., Radjabzadeh, D., Saykin, A.J., Shi, L., Sproviero, W., Winchester, L., Yang, Y., Nevado-Holgado, A.J., Kastenmüller, G., Kaddurah-Daouk, R., van Duijn, C.M., 2023. Interplay of metabolome and gut microbiome in individuals with major depressive disorder vs control individuals. JAMA Psychiatry 80, 597–609. https://doi.org/10.1001/jamapsychiatry.2023.0685.

Aroney, S.T.N., Newell, R.J.P., Nissen, J., Camargo, A.P., Tyson, G.W., Woodcroft, B.J., 2024. CoverM: read coverage calculator for metagenomics. Retrieved on 8 October 2024 from: https://github.com/wwood/CoverM.

Bhattacharyya, S., Ahmed, A.T., Arnold, M., Liu, D., Luo, C., Zhu, H., Mahmoudiandehkordi, S., Neavin, D., Louie, G., Dunlop, B.W., Frye, M.A., Wang, L., Weinshilboum, R.M., Krishnan, R.R., Rush, A.J., Kaddurah-Daouk, R., 2019. Metabolomic signature of exposure and response to citalopram/escitalopram in depressed outpatients. Translational Psychiatry 9, 173. https://doi.org/10.1038/s41398-019-0507-5.

Bortolotti, M., Polito, L., Battelli, M.G., Bolognesi, A., 2021. Xanthine oxidoreductase: one enzyme for multiple physiological tasks. Redox Biology 41, 101882. https://doi.org/10.1016/j.redox.2021.101882.

Bowers, R.M., Kyrpides, N.C., Stepanauskas, R., Harmon-Smith, M., Doud, D., Reddy, T.B.K., Schulz, F., Jarett, J., Rivers, A.R., Eloe-Fadrosh, E.A., Tringe, S.G., Ivanova, N. N., Copeland, A., Clum, A., Becraft, E.D., Malmstrom, R.R., Birren, B., Podar, M., Bork, P., Weinstock, G.M., Garrity, G.M., Dodsworth, J.A., Yooseph, S., Sutton, G., Glöckner, F.O., Gilbert, J.A., Nelson, W.C., Hallam, S.J., Jungbluth, S.P., Ettema, T.J. G., Tighe, S., Konstantinidis, K.T., Liu, W.-T., Baker, B.J., Rattei, T., Eisen, J.A., Hedlund, B., McMahon, K.D., Fierer, N., Knight, R., Finn, R., Cochrane, G., Karsch-Mizrachi, I., Tyson, G.W., Rinke, C., Lapidus, A., Meyer, F., Yilmaz, P., Parks, D.H., Murat Eren, A., Schriml, L., Banfield, J.F., Hugenholtz, P., Woyke, T., 2017. Minimum information about a single amplified genome (MISAG) and a metagenome-assembled genome (MIMAG) of bacteria and archaea. Nature Biotechnology 35, 725–731. https://doi.org/10.1038/nbt.3893.

Camp Montoro, J., Boyle, L.A., Solà-Oriol, D., Muns, R., Gasa, J., Garcia Manzanilla, E., 2021. Effect of space allowance and mixing on growth performance and body lesions of grower-finisher pigs in pens with a single wet-dry feeder. Porcine Health Management 7, 7. https://doi.org/10.1186/s40813-020-00187-7.

Casto-Rebollo, C., Argente, M.J., García, M.L., Blasco, A., Ibáñez-Escriche, N., 2023. Effect of environmental variance-based resilience selection on the gut metabolome of rabbits. Genetics Selection Evolution 55, 15. https://doi.org/10.1186/s12711-023-00791-5.

Chaumeil, P.-A., Mussig, A.J., Hugenholtz, P., Parks, D.H., 2020. GTDB-Tk: a toolkit to classify genomes with the Genome Taxonomy Database. Bioinformatics 36, 1925–1927. https://doi.org/10.1093/bioinformatics/btz848.

Chen, H., Peng, L., Pérez de Nanclares, M., Trudeau, M.P., Yao, D., Cheng, Z., Urriola, P. E., Mydland, L.T., Shurson, G.C., Overland, M., Chen, C., 2019. Identification of sinapine-derived choline from a rapeseed diet as a source of serum trimethylamine N-oxide in pigs. Journal of Agricultural and Food Chemistry 67, 7748–7754. https://doi.org/10.1021/acs.jafc.9b02950.

Cheung, E.C., Vousden, K.H., 2022. The role of ROS in tumour development and progression. Nature Reviews Cancer 22, 280–297. https://doi.org/10.1038/s41568-021-00435-0.

Chklovski, A., Parks, D.H., Woodcroft, B.J., Tyson, G.W., 2023. CheckM2: a rapid, scalable and accurate tool for assessing microbial genome quality using machine learning. Nature Methods 20, 1203–1212. https://doi.org/10.1038/s41592-023-01940-w.

Christensen, D.G., Xie, X., Basisty, N., Byrnes, J., McSweeney, S., Schilling, B., Wolfe, A. J., 2019. Post-translational protein acetylation: an elegant mechanism for bacteria to dynamically regulate metabolic functions. Frontiers in Microbiology 10, 1604. https://doi.org/10.3389/fmicb.2019.01604.

Clavell-Sansalvador, A., Río-López, R., González-Rodríguez, O., García-Gil, L.J., Xifró, X., Zigovski, G., Ochoteco-Asensio, J., Ballester, M., Dalmau, A., Ramayo-Caldas, Y., 2024. Effect of group mixing and available space on performance, feeding behavior, and fecal microbiota composition during the growth period of pigs. Animals 14, 2704. https://doi.org/10.3390/ani14182704.

Davenport, M.D., Tiefenbacher, S., Lutz, C.K., Novak, M.A., Meyer, J.S., 2006. Analysis of endogenous cortisol concentrations in the hair of rhesus macaques. General and Comparative Endocrinology 147, 255–261. https://doi.org/10.1016/j.ygcen.2006.01.005.

Escribano, D., Gutiérrez, A.M., Tecles, F., Cerón, J.J., 2015. Changes in saliva biomarkers of stress and immunity in domestic pigs exposed to a psychosocial stressor. Research in Veterinary Science 102, 38–44. https://doi.org/10.1016/j.rvsc.2015.07.013.

Ewels, P.A., Peltzer, A., Fillinger, S., Patel, H., Alneberg, J., Wilm, A., Garcia, M.U., Di Tommaso, P., Nahnsen, S., 2020. The nf-core framework for community-curated bioinformatics pipelines. Nature Biotechnology 38, 276–278. https://doi.org/10.1038/s41587-020-0439-x.

Fan, S., Kind, T., Cajka, T., Hazen, S.L., Tang, W.H.W., Kaddurah-Daouk, R., Irvin, M.R., Arnett, D.K., Barupal, D.K., Fiehn, O., 2019. Systematic error removal using random forest for normalizing large-scale untargeted lipidomics data. Analytical Chemistry 91, 3590–3596. https://doi.org/10.1021/acs.analchem.8b05592.

Friedman, J.H., Hastie, T., Tibshirani, R., 2010. Regularization paths for generalized linear models via coordinate descent. Journal of Statistical Software 33, 1–22. https://doi.org/10.18637/jss.v033.i01.

Fu, L., Li, H., Liang, T., Zhou, B., Chu, Q., Schinckel, A.P., Yang, X., Zhao, R., Li, P., Huang, R., 2016. Stocking density affects welfare indicators of growing pigs of different group sizes after regrouping. Applied Animal Behaviour Science 174, 42–50. https://doi.org/10.1016/j.applanim.2015.10.002.

Galli, M.C., Lagoda, M.E., Gottardo, F., Contiero, B., Boyle, L.A., 2023. The role of environmental enrichment and back fat depth in the intensity of aggressive behavior performed by sows during the establishment of the dominance hierarchy. Animals : An Open Access Journal from MDPI 13, 825. https://doi.org/10.3390/ani13050825.

Gimsa, U., Tuchscherer, M., Kanitz, E., 2018. Psychosocial stress and Immunity—what can we learn from pig studies? Frontiers in Behavioral Neuroscience 12, 64. https://doi.org/10.3389/fnbeh.2018.00064.

Greenacre, M., Martínez-Álvaro, M., Blasco, A., 2021. Compositional data analysis of microbiome and any-omics datasets: a validation of the additive logratio transformation. Frontiers in Microbiology 12, 727398. https://doi.org/10.3389/fmicb.2021.727398.

Gul, A., Kunwar, B., Mazhar, M., Perveen, K., Simjee, S.U., 2017. N-(2-Hydroxyphenyl)acetamide: a novel suppressor of RANK/RANKL pathway in collagen-induced arthritis model in rats. Inflammation 40, 1177–1190. https://doi.org/10.1007/s10753-017-0561-1.

Guo, S., Wang, Y., Wang, W., Hu, H., Zhang, X., 2020. Identification of new arylamine N-acetyltransferases and enhancing 2-acetamidophenol production in *Pseudomonas chlororaphis* HT66. Microbial Cell Factories 19, 105. https://doi.org/10.1186/s12934-020-01364-7.

Ha, E.-M., Lee, K.-A., Seo, Y.Y., Kim, S.-H., Lim, J.-H., Oh, B.-H., Kim, J., Lee, W.-J., 2009. Coordination of multiple dual oxidase–regulatory pathways in responses to commensal and infectious microbes in drosophila gut. Nature Immunology 10, 949–957. https://doi.org/10.1038/ni.1765.

Hao, B., Chen, K., Zhai, L., Liu, M., Liu, B., Tan, M., 2024. Substrate and functional diversity of protein lysine post-translational modifications. Genomics, Proteomics & Bioinformatics 22, qzae019. https://doi.org/10.1093/gpbjnl/qzae019.

He, Y., Maltecca, C., Tiezzi, F., 2021. Potential use of gut microbiota composition as a biomarker of heat stress in monogastric species: a review. Animals: An Open Access Journal from MDPI 11, 1833. https://doi.org/10.3390/ani11061833.

Heimbürge, S., Kanitz, E., Otten, W., 2019. The use of hair cortisol for the assessment of stress in animals. General and Comparative Endocrinology 270, 10–17. https://doi.org/10.1016/j.ygcen.2018.09.016.

Jiang, L., Han, D., Hao, Y., Song, Z., Sun, Z., Dai, Z., 2024. Linking serotonin homeostasis to gut function: nutrition, gut microbiota and beyond. Critical Reviews in Food Science and Nutrition 64, 7291–7310. https://doi.org/10.1080/10408398.2023.2183935.

Kaczmarek, J.L., Thompson, S.V., Holscher, H.D., 2017. Complex interactions of circadian rhythms, eating behaviors, and the gastrointestinal microbiota and their potential impact on health. Nutrition Reviews 75, 673–682. https://doi.org/10.1093/nutrit/nux036.

Kanehisa, M., Goto, S., 2000. KEGG: kyoto encyclopedia of genes and genomes. Nucleic Acids Research 28, 27–30. https://doi.org/10.1093/nar/28.1.27.

Kang, D.D., Li, F., Kirton, E., Thomas, A., Egan, R., An, H., Wang, Z., 2019. MetaBAT 2: an adaptive binning algorithm for robust and efficient genome reconstruction from metagenome assemblies. PeerJ 7, e7359.

Kick, A.R., Tompkins, M.B., Almond, G.W., 2011. Stress and immunity in the pig. CABI Reviews 2011, 1–17. https://doi.org/10.1079/PAVSNNR20116018.
Kim, E.-K., Lee, K.-A., Hyeon, D.Y., Kyung, M., Jun, K.-Y., Seo, S.H., Hwang, D., Kwon, Y., Lee, W.-J., 2020. Bacterial nucleoside catabolism controls quorum sensing and commensal-to-pathogen transition in the *Drosophila* gut. Cell Host & Microbe 27, 345–357.e6. https://doi.org/10.1016/j.chom.2020.01.025.
Krakau, S., Straub, D., Gourlé, H., Gabernet, G., Nahnsen, S., 2022. nf-core/mag: a best-practice pipeline for metagenome hybrid assembly and binning. NAR Genomics and Bioinformatics 4, lqac007. https://doi.org/10.1093/nargab/lqac007.
Lee, K.-A., Kim, S.-H., Kim, E.-K., Ha, E.-M., You, H., Kim, B., Kim, M.-J., Kwon, Y., Ryu, J.-H., Lee, W.-J., 2013. Bacterial-derived uracil as a modulator of mucosal immunity and gut-microbe homeostasis in *Drosophila*. Cell 153, 797–811. https://doi.org/10.1016/j.cell.2013.04.009.
Lee, K.-A., Kim, B., Bhin, J., Kim, D.H., You, H., Kim, E.-K., Kim, S.-H., Ryu, J.-H., Hwang, D., Lee, W.-J., 2015. Bacterial uracil modulates *Drosophila* DUOX-dependent gut immunity via hedgehog-induced signaling endosomes. Cell Host & Microbe 17, 191–204. https://doi.org/10.1016/j.chom.2014.12.012.
Lee, K.-A., Cho, K.-C., Kim, B., Jang, I.-H., Nam, K., Kwon, Y.E., Kim, M., Hyeon, D.Y., Hwang, D., Seol, J.-H., Lee, W.-J., 2018. Inflammation-modulated metabolic reprogramming is required for DUOX-dependent gut immunity in *Drosophila*. Cell Host & Microbe 23, 338–352.e5. https://doi.org/10.1016/j.chom.2018.01.011.
Leigh, S.-J., Uhlig, F., Wilmes, L., Sanchez-Diaz, P., Gheorghe, C.E., Goodson, M.S., Kelley-Loughnane, N., Hyland, N.P., Cryan, J.F., Clarke, G., 2023. The impact of acute and chronic stress on gastrointestinal physiology and function: a microbiota–gut–brain axis perspective. The Journal of Physiology 601, 4491–4538. https://doi.org/10.1113/JP281951.
Li, Y., Guo, Y., Wen, Z., Jiang, X., Ma, X., Han, X., 2018. Weaning stress perturbs gut microbiome and its metabolic profile in piglets. Scientific Reports 8, 18068. https://doi.org/10.1038/s41598-018-33649-8.
Li, Y., Li, J., Su, Q., Liu, Y., 2019. Sinapine reduces non-alcoholic fatty liver disease in mice by modulating the composition of the gut microbiota. Food & Function 10, 3637–3649. https://doi.org/10.1039/c9fo00195f.
Li, D., Liu, C.-M., Luo, R., Sadakane, K., Lam, T.-W., 2015. MEGAHIT: an ultra-fast single-node solution for large and complex metagenomics assembly via succinct de Bruijn graph. Bioinformatics (Oxford, England) 31, 1674–1676. https://doi.org/10.1093/bioinformatics/btv033.
Li, Y., Xu, Y.-J., Tan, C.P., Liu, Y., 2022. Sinapine improves LPS-induced oxidative stress in hepatocytes by down-regulating MCJ protein expression. Life Sciences 306, 120828. https://doi.org/10.1016/j.lfs.2022.120828.
Liu, Z., Ling, Y., Peng, Y., Han, S., Ren, Y., Jing, Y., Fan, W., Su, Y., Mu, C., Zhu, W., 2023. Regulation of serotonin production by specific microbes from piglet gut. Journal of Animal Science and Biotechnology 14, 111. https://doi.org/10.1186/s40104-023-00903-7.
Liu, P., Liu, Z., Wang, J., Wang, J., Gao, M., Zhang, Y., Yang, C., Zhang, A., Li, G., Li, X., Liu, S., Liu, L., Sun, N., Zhang, K., 2024. Immunoregulatory role of the gut microbiota in inflammatory depression. Nature Communications 15, 3003. https://doi.org/10.1038/s41467-024-47273-w.
Liu, Y., Yin, H.-L., Li, C., Jiang, F., Zhang, S.-J., Zhang, X.-R., Li, Y.-L., 2020. Sinapine thiocyanate ameliorates vascular endothelial dysfunction in hypertension by inhibiting activation of the NLRP3 inflammasome. Frontiers in Pharmacology 11, 620159. https://doi.org/10.3389/fphar.2020.620159.
Majzoub, M.E., Luu, L.D.W., Haifer, C., Paramsothy, S., Borody, T.J., Leong, R.W., Thomas, T., Kaakoush, N.O., 2024. Refining microbial community metabolic models derived from metagenomics using reference-based taxonomic profiling. mSystems 9, e00746-24. https://doi.org/10.1128/msystems.00746-24.
Martin, A.M., Young, R.L., Leong, L., Rogers, G.B., Spencer, N.J., Jessup, C.F., Keating, D. J., 2017. The diverse metabolic roles of peripheral serotonin. Endocrinology 158, 1049–1063. https://doi.org/10.1210/en.2016-1839.
Martínez-Miró, S., Tecles, F., Ramón, M., Escribano, D., Hernández, F., Madrid, J., Orengo, J., Martínez-Subiela, S., Manteca, X., Cerón, J.J., 2016. Causes, consequences and biomarkers of stress in swine: an update. BMC Veterinary Research 12, 171. https://doi.org/10.1186/s12917-016-0791-8.
Meese, G.B., Ewbank, R., 1973. The establishment and nature of the dominance hierarchy in the domesticated pig. Animal Behaviour 21, 326–334. https://doi.org/10.1016/S0003-3472(73)80074-0.
Menneson, S., Ménicot, S., Ferret-Bernard, S., Guérin, S., Romé, V., Le Normand, L., Randuineau, G., Gambarota, G., Noirot, V., Etienne, P., Coquery, N., Val-Laillet, D., 2019. Validation of a psychosocial chronic stress model in the pig using a multidisciplinary approach at the gut-brain and behavior levels. Frontiers in Behavioral Neuroscience 13, 161. https://doi.org/10.3389/fnbeh.2019.00161.
Mittasch, J., Mikolajewski, S., Breuer, F., Strack, D., Milkowski, C., 2010. Genomic microstructure and differential expression of the genes encoding UDP-glucose: sinapate glucosyltransferase (UGT84A9) in oilseed rape (*Brassica napus*). TAG. Theoretical and applied genetics. Theoretische Und Angewandte Genetik 120, 1485–1500. https://doi.org/10.1007/s00122-010-1270-4.
Moretti, C.H., Grasset, E., Zhu, J., Yang, G., Olofsson, L.E., Khan, M.T., Bergh, P.-O., Oh, J.-H., Lundqvist, A., van Gils, T., Krämer, M., Olsson, L.M., Patel, P., Mitteregger, M., Monges, D.E., Dwibedi, C., Krautkramer, K.A., Koopman, N., Henricsson, M., Macpherson, A.J., Schwartz, T., Grompone, G., van Pijkeren, J.-P., Tremaroli, V., Roos, S., Simrén, M., Bäckhed, F., 2025. Identification of human gut bacteria that produce bioactive serotonin and promote colonic innervation. Cell Reports 44, 116434. https://doi.org/10.1016/j.celrep.2025.116434.
Nannoni, E., Martelli, G., Rubini, G., Sardi, L., 2019. Effects of increased space allowance on animal welfare, meat and ham quality of heavy pigs slaughtered at 160Kg. PLoS One 14, e0212417. https://doi.org/10.1371/journal.pone.0212417.
Nguyen, T.Q., Martínez-Álvaro, M., Lima, J., Auffret, M.D., Rutherford, K.M.D., Simm, G., Dewhurst, R.J., Baima, E.T., Roehe, R., 2023. Identification of intestinal and fecal microbial biomarkers using a porcine social stress model. Frontiers in Microbiology 14, 1197371. https://doi.org/10.3389/fmicb.2023.1197371.
Nutrient Requirements of Swine: Eleventh ed., 2012. National Academies Press, Washington, DC, USA. https://doi.org/10.17226/13298.
Olm, M.R., Brown, C.T., Brooks, B., Banfield, J.F., 2017. dRep: a tool for fast and accurate genomic comparisons that enables improved genome recovery from metagenomes through de-replication. The ISME Journal 11, 2864–2868. https://doi.org/10.1038/ismej.2017.126.
Papatsiros, V.G., Maragkakis, G., Papakonstantinou, G.I., 2024. Stress biomarkers in pigs: current insights and clinical application. Veterinary Sciences 11, 640. https://doi.org/10.3390/vetsci11120640.
Peng, H., Qiu, J.-Q., Zhou, Q., Zhang, Y., Chen, Q., Yin, Y., Su, W., Yu, S., Wang, Y., Cai, Y., Gu, M., Zhang, H., Sun, Q., Hu, G., Wu, Y., Liu, J., Chen, S., Zhu, Z.-J., Song, X., Zhou, J., 2023. Intestinal epithelial dopamine receptor signaling drives sex-specific disease exacerbation in a mouse model of multiple sclerosis. Immunity 56, 2773–2789.e8. https://doi.org/10.1016/j.immuni.2023.10.016.
Perveen, K., Hanif, F., Jawed, H., Jamall, S., Simjee, S.U., 2014. N-(2-hydroxy phenyl) acetamide: a novel suppressor of Toll-like receptors (TLR-2 and TLR-4) in adjuvant-induced arthritic rats. Molecular and Cellular Biochemistry 394, 67–75. https://doi.org/10.1007/s11010-014-2082-7.
Prims, S., Vanden Hole, C., Van Cruchten, S., Van Ginneken, C., Van Ostade, X., Casteleyn, C., 2019. Hair or salivary cortisol analysis to identify chronic stress in piglets? Veterinary Journal 252, 105357. https://doi.org/10.1016/j.tvjl.2019.105357.
Principi, N., Esposito, S., 2016. Gut microbiota and central nervous system development. Journal of Infection 73, 536–546. https://doi.org/10.1016/j.jinf.2016.09.010.
Proudfoot, K., Habing, G., 2015. Social stress as a cause of diseases in farm animals: current knowledge and future directions. Veterinary Journal 206, 15–21. https://doi.org/10.1016/j.tvjl.2015.05.024.
R Core Team, 2021. R: The R Project for Statistical Computing. R Foundation for Statistical Computing, Vienna, Austria.
Ravi, M., Miller, A.H., Michopoulos, V., 2021. The immunology of stress and the impact of inflammation on the brain and behaviour. Bjpsych Advances 27, 158–165. https://doi.org/10.1192/bja.2020.82.
Rohart, F., Gautier, B., Singh, A., Cao, K.-A.-L., 2017. mixOmics: an R package for 'omics feature selection and multiple data integration. PLoS Computational Biology 13, e1005752. https://doi.org/10.1371/journal.pcbi.1005752.
Russell, G., Lightman, S., 2019. The human stress response. Nature Reviews Endocrinology 15, 525–534. https://doi.org/10.1038/s41574-019-0228-0.
Sánchez, J., Matas, M., Ibáñez-López, F.J., Hernández, I., Sotillo, J., Gutiérrez, A.M., 2022. The connection between stress and Immune status in pigs: a first salivary analytical panel for disease differentiation. Frontiers in Veterinary Science 9, 881435. https://doi.org/10.3389/fvets.2022.881435.
Shaffer, M., Borton, M.A., McGivern, B.B., Zayed, A.A., La Rosa, S.L., Solden, L.M., Liu, P., Narrowe, A.B., Rodríguez-Ramos, J., Bolduc, B., Gazitúa, M.C., Daly, R.A., Smith, G.J., Vik, D.R., Pope, P.B., Sullivan, M.B., Roux, S., Wrighton, K.C., 2020. DRAM for distilling microbial metabolism to automate the curation of microbiome function. Nucleic Acids Research 48, 8883–8900. https://doi.org/10.1093/nar/gkaa621.
Shaw, J., Yu, Y.W., 2023. Metagenome profiling and containment estimation through abundance-corrected k-mer sketching with sylph. bioRxiv. Retrieved on 7 March 2025 from: http://biorxiv.org/content/early/2023/11/20/2023.11.20.567879.abstract.
Siddiqui, R.A., Simjee, S.U., Kabir, N., Ateeq, M., Shah, M.R., Hussain, S.S., 2019. N-(2-hydroxyphenyl)acetamide and its gold nanoparticle conjugation prevent glycerol-induced acute kidney injury by attenuating inflammation and oxidative injury in mice. Molecular and Cellular Biochemistry 450, 43–52. https://doi.org/10.1007/s11010-018-3371-3.
Silva, Y.P., Bernardi, A., Frozza, R.L., 2020. The role of short-chain fatty acids from gut microbiota in gut-brain communication. Frontiers in Endocrinology 11, 25. https://doi.org/10.3389/fendo.2020.00025.
Strandwitz, P., 2018. Neurotransmitter modulation by the gut microbiota. Brain Research 1693, 128–133. https://doi.org/10.1016/j.brainres.2018.03.015.
Sumner, L.W., Amberg, A., Barrett, D., Beale, M.H., Beger, R., Daykin, C.A., Fan, T.-W.-M., Fiehn, O., Goodacre, R., Griffin, J.L., Hankemeier, T., Hardy, N., Harnly, J., Higashi, R., Kopka, J., Lane, A.N., Lindon, J.C., Marriott, P., Nicholls, A.W., Reily, M. D., Thaden, J.J., Viant, M.R., 2007. Proposed minimum reporting standards for chemical analysis Chemical Analysis Working Group (CAWG) Metabolomics Standards Initiative (MSI). Metabolomics: Official Journal of the Metabolomic Society 3, 211–221. https://doi.org/10.1007/s11306-007-0082-2.
Svoboda, M., Nemeckova, M., Medkova, D., Sardi, L., Hodkovicova, N., 2024. Non-invasive methods for analysing pig welfare biomarkers. Veterinarni Medicina 69, 137–155. https://doi.org/10.17221/17/2024-VETMED.
Tang, S., Xie, J., Fang, W., Wen, X., Yin, C., Meng, Q., Zhong, R., Chen, L., Zhang, H., 2022. Chronic heat stress induces the disorder of gut transport and immune function associated with endoplasmic reticulum stress in growing pigs. Animal Nutrition (zhongguo Xu Mu Shou Yi Xue Hui) 11, 228–241. https://doi.org/10.1016/j.aninu.2022.08.008.
Tibshirani, R., 2011. Regression shrinkage and selection via the lasso: a retrospective. Journal of the Royal Statistical Society: Series B (Statistical Methodology) 73, 273–282. https://doi.org/10.1111/j.1467-9868.2011.00771.x.

Turner, S.P., Ewen, M., Rooke, J.A., Edwards, S.A., 2000. The effect of space allowance on performance, aggression and immune competence of growing pigs housed on straw deep-litter at different group sizes. Livestock Production Science 66, 47–55. https://doi.org/10.1016/S0301-6226(00)00159-7.

Ueda, A., Attila, C., Whiteley, M., Wood, T.K., 2009. Uracil influences quorum sensing and biofilm formation in *Pseudomonas aeruginosa* and fluorouracil is an antagonist. Microbial Biotechnology 2, 62–74. https://doi.org/10.1111/j.1751-7915.2008.00060.x.

Uritskiy, G.V., DiRuggiero, J., Taylor, J., 2018. MetaWRAP—a flexible pipeline for genome-resolved metagenomic data analysis. Microbiome 6, 158. https://doi.org/10.1186/s40168-018-0541-1.

Valdés, A., Moreno, L.O., Rello, S.R., Orduña, A., Bernardo, D., Cifuentes, A., 2022. Metabolomics study of COVID-19 patients in four different clinical stages. Scientific Reports 12, 1650. https://doi.org/10.1038/s41598-022-05667-0.

Valles-Colomer, M., Falony, G., Darzi, Y., Tigchelaar, E.F., Wang, J., Tito, R.Y., Schiweck, C., Kurilshikov, A., Joossens, M., Wijmenga, C., Claes, S., Van Oudenhove, L., Zhernakova, A., Vieira-Silva, S., Raes, J., 2019. The neuroactive potential of the human gut microbiota in quality of life and depression. Nature Microbiology 4, 623–632. https://doi.org/10.1038/s41564-018-0337-x.

Vasquez, R., Oh, J.K., Song, J.H., Kang, D.-K., 2022. Gut microbiome-produced metabolites in pigs: a review on their biological functions and the influence of probiotics. Journal of Animal Science and Technology 64, 671–695. https://doi.org/10.5187/jast.2022.e58.

Vourlaki, I.-T., Rio-Lopez, R., Clavell-Sansalvador, A., Ramírez-Ayala, L.C., Ballester, M., Sanchez, J.P., Piles, M., Quintanilla, R., da Fonseca de Oliveira, A.C., Costa, L.B., Dalmau, A., Ramayo-Caldas, Y., 2025. Co-occurring microbial guilds in pig fecal microbiota: key drivers and effects on host performance. Genetics Selection Evolution 57, 27. https://doi.org/10.1186/s12711-025-00979-x.

Wang, Y., Chen, Y., Zhang, A., Chen, K., Ouyang, P., 2023b. Advances in the microbial synthesis of the neurotransmitter serotonin. Applied Microbiology and Biotechnology 107, 4717–4725. https://doi.org/10.1007/s00253-023-12584-3.

Wang, T., Wang, X.-W., Lee-Sarwar, K.A., Litonjua, A.A., Weiss, S.T., Sun, Y., Maslov, S., Liu, Y.-Y., 2023a. Predicting metabolomic profiles from microbial composition through neural ordinary differential equations. Nature Machine Intelligence 5, 284–293. https://doi.org/10.1038/s42256-023-00627-3.

Wu, Y.-W., Simmons, B.A., Singer, S.W., 2016. MaxBin 2.0: an automated binning algorithm to recover genomes from multiple metagenomic datasets. Bioinformatics 32, 605–607. https://doi.org/10.1093/bioinformatics/btv638.

Xie, Y., Wang, C., Zhao, D., Wang, C., Li, C., 2020. Dietary proteins regulate serotonin biosynthesis and catabolism by specific gut microbes. Journal of Agricultural and Food Chemistry 68, 5880–5890. https://doi.org/10.1021/acs.jafc.0c00832.

Yang, S., Lian, G., 2020. ROS and diseases: role in metabolism and energy supply. Molecular and Cellular Biochemistry 467, 1–12. https://doi.org/10.1007/s11010-019-03667-9.

Yano, J.M., Yu, K., Donaldson, G.P., Shastri, G.G., Ann, P., Ma, L., Nagler, C.R., Ismagilov, R.F., Mazmanian, S.K., Hsiao, E.Y., 2015. Indigenous bacteria from the gut microbiota regulate host serotonin biosynthesis. Cell 161, 264–276. https://doi.org/10.1016/j.cell.2015.02.047.

Yin, J., Li, Y., Han, H., Liu, Z., Zeng, X., Li, T., Yin, Y., 2018. Long-term effects of lysine concentration on growth performance, intestinal microbiome, and metabolic profiles in a pig model. Food & Function 9, 4153–4163. https://doi.org/10.1039/c8fo00973b.

Yu, D., Huang, X., Zou, C., Li, B., Duan, J., Yin, Q., 2016. Isolation and identification of sinapine-degrading bacteria from the intestinal tract of laying hens. Animal Nutrition (zhongguo Xu Mu Shou Yi Xue Hui) 2, 57–62. https://doi.org/10.1016/j.aninu.2016.02.002.

Zhao, Q., Baranova, A., Cao, H., Zhang, F., 2024. Gut microbiome and major depressive disorder: insights from two-sample Mendelian randomization. BMC Psychiatry 24, 493. https://doi.org/10.1186/s12888-024-05942-6.

Zheng, X., Xu, L., Tang, Q., Shi, K., Wang, Z., Shi, L., Ding, Y., Yin, Z., Zhang, X., 2024. Integrated metagenomic and metabolomics profiling reveals key gut microbiota and metabolites associated with weaning stress in piglets. Genes 15, 970. https://doi.org/10.3390/genes15080970.

Zhou, M., Fan, Y., Xu, L., Yu, Z., Wang, S., Xu, H., Zhang, J., Zhang, L., Liu, W., Wu, L., Yu, J., Yao, H., Wang, J., Gao, R., 2023. Microbiome and tryptophan metabolomics analysis in adolescent depression: roles of the gut microbiota in the regulation of tryptophan-derived neurotransmitters and behaviors in human and mice. Microbiome 11, 145. https://doi.org/10.1186/s40168-023-01589-9.

Zuffa, S., Schmid, R., Bauermeister, A.P., Gomes, P.W., Caraballo-Rodriguez, A.M., El Abiead, Y., Aron, A.T., Gentry, E.C., Zemlin, J., Meehan, M.J., Avalon, N.E., Cichewicz, R.H., Buzun, E., Terrazas, M.C., Hsu, C.-Y., Oles, R., Ayala, A.V., Zhao, J., Chu, H., Kuijpers, M.C.M., Jackrel, S.L., Tugizimana, F., Nephali, L.P., Dubery, I.A., Madala, N.E., Moreira, E.A., Costa-Lotufo, L.V., Lopes, N.P., Rezende-Teixeira, P., Jimenez, P.C., Rimal, B., Patterson, A.D., Traxler, M.F., Pessotti, R. de C., Alvarado-Villalobos, D., Tamayo-Castillo, G., Chaverri, P., Escudero-Leyva, E., Quiros-Guerrero, L.-M., Bory, A.J., Joubert, J., Rutz, A., Wolfender, J.-L., Allard, P.-M., Sichert, A., Pontrelli, S., Pullman, B.S., Bandeira, N., Gerwick, W.H., Gindro, K., Massana-Codina, J., Wagner, B.C., Forchhammer, K., Petras, D., Aiosa, N., Garg, N., Liebeke, M., Bourceau, P., Kang, K.B., Gadhavi, H., de Carvalho, L.P.S., Silva dos Santos, M., Pérez-Lorente, A.I., Molina-Santiago, C., Romero, D., Franke, R., Brönstrup, M., Ponce, Vera, de León, A., Pope, P.B., La Rosa, S.L., La Barbera, G., Roager, H.M., Laursen, M.F., Hammerle, F., Siewert, B., Peintner, U., Licona-Cassani, C., Rodriguez-Orduña, L., Rampler, E., Hildebrand, F., Koellensperger, G., Schoeny, H., Hohenwallner, K., Panzenboeck, L., Gregor, R., O'Neill, E.C., Roxborough, E.T., Odoi, J., Bale, N.J., Ding, S., Sinninghe Damsté, J.S., Guan, X. L., Cui, J.J., Ju, K.-S., Silva, D.B., Silva, F.M.R., da Silva, G.F., Koolen, H.H.F., Grundmann, C., Clement, J.A., Mohimani, H., Broders, K., McPhail, K.L., Ober-Singleton, S.E., Rath, C.M., McDonald, D., Knight, R., Wang, M., Dorrestein, P. C., 2024. microbeMASST: a taxonomically informed mass spectrometry search tool for microbial metabolomics data. Nature Microbiology 9, 336–345. https://doi.org/10.1038/s41564-023-01575-9.